

Near-Earth Objects

A threat for Earth? – Or: NEOs for engineers and physicists



IMAGE CREDIT: ESA - AOES MEDIALAB

PROF. D. KOSCHNY

15 APR 2024

1. Table of Contents

2. Introduction.....	5
3. Historical background.....	6
4. Where do asteroids come from?	7
5. Terminology	9
5.1 Asteroids and comets.....	9
5.2 Main-belt objects	10
5.3 Near-Earth objects	10
5.4 Atens, Apollos, Amors, Atiras.....	11
5.5 Mean Orbital Intersection Distance	12
5.6 Magnitude.....	12
5.7 Johnson-Cousins filter bands.....	13
5.8 Absolute magnitude	14
5.9 Albedo.....	14
5.10 Potentially Hazardous Objects.....	14
5.11 Asteroid families.....	14
5.12 Nu6 resonance	15
5.13 Observatory code.....	16
5.14 Conjunction, elongation, and opposition.....	16
6. From observations to measurements – the current state of near-Earth object observations.....	16
7. Ongoing ground-based survey programs.....	19
7.1 Catalina Sky Survey	20
7.2 Pan-STARRS.....	20
7.3 La Sagra Sky Survey	20
7.4 Teide Observatory Tenerife Asteroid Survey.....	21
.....	22
8. Detection limits for asteroids.....	22
8.1 Introduction.....	22
8.2 Brightness of the asteroid	22
8.3 Telescope throughput.....	23
8.4 Detection in a CCD camera	25
9. Determining an asteroid’s position from an image.....	29
10. Follow-up – an important activity to keep track of where the objects are	30
11. Orbit determination and first impact warning	31
11.1 Introduction.....	31
11.2 Converting celestial coordinates to inertial vectors.....	31
11.3 The position of the Earth as a function of time	32
11.4 Converting to a state vector	33

11.5	Applying the method of Herget to estimate radius and velocity vectors.....	33
11.6	Convert these to orbital elements	34
11.7	Non-gravitational forces	36
11.8	Keyholes	36
11.9	Propagating orbits to generate impact warnings.....	37
11.9.1	Torino scale	37
11.9.2	Palermo scale	38
11.9.3	Megaton/kiloton TNT	39
11.10	Orbit propagation.....	39
11.11	The Yarkovsky effect	39
12.	Physical properties characterization	40
12.1	Obtaining the observations	42
12.2	Measuring light curves	42
12.3	Deriving the rotation period.....	43
12.4	Spectroscopic observations.....	43
12.5	Temperature of an asteroid	43
12.6	Thermal observations.....	44
12.7	Radar observations.....	45
13.	Impact probabilities and consequences	45
14.	Decision process for impact threat mitigation	46
15.	The Planetary Defence Office within the Space Safety programme of the European Space Agency.....	48
15.1	Introduction.....	48
15.2	What is Space Safety?	48
15.3	Tasks of the programme	49
15.4	Detailed tasks of the Planetary Defence Office	49
16.	Asteroid deflection techniques – avoiding an impact.....	51
16.1	Introduction.....	51
16.2	Impulsive deflection	51
16.2.1	Kinetic impactor	51
16.2.2	Nuclear methods	54
16.3	Slow-push or –pull techniques.....	54
16.3.1	Gravity tractor.....	54
16.3.2	Ion-beam shepherd.....	54
16.4	Other concepts	54
17.	References.....	56
18.	Acronyms.....	57
19.	Tasks	60
19.1	Task 1 - Telescope image scale	60

19.2	Task 2 - Telescope sensitivity.....	60
19.3	Task 3 - Palermo scale values.....	60
19.4	Task 4: Temperature of an asteroid	60
19.5	Task 5: Radar equation	60
19.6	Task 6: Asteroid movement.....	60
19.7	Task 7: Position of an asteroid.....	61
19.8	Task 8: The Apophis story.....	61
19.9	Task 9: Apophis deflection.....	61
19.10	Task 10: The Deep Impact mission	61
19.11	Task 11: Impact deflection demonstration using a binary asteroid	61
19.12	Task 12: The Ion-Beam Shepard	61

2. Introduction

Near-Earth objects are asteroids or comets that come close to the Earth. Only in the last few decades people started to worry about these objects being a risk to life on Earth. The most dramatic event attributed to the impact of an asteroid surely is the so-called K-Pg event (Alvarez et al. 1980). This was a presumed impact about 65 to 66 Million years ago, at the boundary of the geological epochs of the Cretaceous and the Paleogene (thus 'K-Pg' – formerly known as K-T boundary, for Cretaceous and Tertiary). It is currently assumed that an asteroid of about 10 km in size hit the Earth at that time. This is the 'Alvarez hypothesis': In 1980, a team of researchers led by physicist Luis Alvarez, his son, geologist Walter Alvarez, and chemists Frank Asaro and Helen Vaughn Michel discovered that sedimentary layers found all over the world at the Cretaceous–Paleogene boundary contain a concentration of iridium hundreds of times greater than normal. This was attributed by them to an large asteroid impact, resulting in the extinction of not only the dinosaurs, but of many other life forms on our planet.

While the first asteroid was discovered over 200 years ago, in 1801, we only realized in the 1980s that the solar system is full of these objects. Many come close to our planet, and until 2024 over 35000 of these so-called near-Earth objects (NEOs) have been discovered. In the last few years, decision makers also realized that these objects pose a real threat to our planet. Unlike earthquakes or tsunamis, we could deflect a potentially impacting asteroid. Thus, even the United Nations now recognizes this threat. Since 2013, two UN-endorsed groups are working on this topic – the International Asteroid Warning Network (IAWN) and the Space Mission Planning Advisory Group (SMPAG).

The US was the first nation to recognize the seriousness of this threat and to implement some guaranteed funding for the discovery and tracking of NEOs. Since 2008, there is also a European programme in place that is dealing with the NEO impact threat. Initially called Europe's Space Situational Awareness programme, the threat of NEOs is now dealt with by the Planetary Defence Office within ESA's Space Safety Programme.

Setting up a NEO programme, which deals with the observation of asteroids and comets, with the computation of orbits, the analysis of impact consequences, and the development of possible mitigation missions, requires both engineers and scientists of many different disciplines. This text aims at giving an overview of near-Earth objects for all those that want to contribute in the future to this interesting challenge.

We first provide a very short overview of the current knowledge on NEOs, then we explain how they are being observed and the risk they pose for our planet. After that, ongoing activities to define decision strategies on what to do in the case of an imminent impact threat are described. Finally, the current activities of the Planetary Defence Office within ESA's Space Safety programme and in particular its near-Earth object segment is outlined.

This text was written as a script for a lecture given at the Technical University of Munich. It thus assumes a reasonable knowledge of mathematics and aerospace engineering. It does not want to replace text books in particular in the field of orbital dynamics as this would be beyond the scope of the lecture. It focusses on aspects typical when dealing with NEOs.

I dedicate this book to Prof. Eduard Igenbergs, my Ph.D. supervisor and mentor. Without him, I would not be teaching a course on my favorite topic at the Technical University of Munich.

3. Historical background

Since several centuries, we know that the Earth is orbiting about the Sun, as one out of several planets. There are eight known planets – Mercury, Venus, Earth, Mars, Jupiter, Saturn, Uranus, and Neptune. Neptune was discovered in the year 1781. Its orbit was such that scientists thought that there may be another planet out there, disturbing Neptune’s orbit. Several astronomers started searching for this disturbing object. In 1801, Giuseppe Piazzi visually discovered an object which turned out not to be in the right orbit for another planet – but it was still a real object. It was called ‘asteroid’ (meaning “like a star”), and Piazzi named it (1) Ceres. In the next decades, a number of asteroids were discovered, all of them too small to really be the ‘missing planet’. Only in 1930, Clyde Tombaugh discovered Pluto, which was – until a decision by the International Astronomical Union in 2008 changed its status – the 9th planet. All other objects were called ‘asteroids’. Those objects that display a coma – a sign for out-gassing volatiles - are called comets.

Until 1891, about 300 asteroids were discovered, all of them visually by observers looking through their telescope with their eye. In that year, 1891, Max Wolf discovered the first asteroid via photography. In the next 20 years, another 300 asteroids were discovered via this technique.

In the mid-20th century, a number of dedicated asteroid surveys were performed. These were mainly performed with wide-angle Schmidt cameras, e.g. the 48” Palomar Schmidt telescope as shown in Figure 1. Until 1990, about 9000 asteroids were known in total. In those years, automated search programs using electronic CCD cameras started. The number of detected asteroids increased dramatically. In the year 2000, almost 90000 objects were known; in 2013 there were around 600000 objects in our catalogues, in 2024 we knew more than 1 million. The book ‘Asteroids – A history’ provides a detailed and well-written summary of the history of asteroid observations (Peebles 2000).

A subset of the asteroid population, those that come close to the Earth, are called near-Earth asteroids (NEAs). Including comets, the population is called near-Earth objects (NEOs). According to the current definition of the International Astronomical Union, NEOs are defined as objects orbiting the Sun with pericenter distances of less than 1.3 au¹. If they cross the path of the Earth in the orbit around the Sun, they pose a threat to our planet. An object with about 40 m diameter exploded in the atmosphere above the Siberian Tunguska area in 1908 and flattened >2000 km² of forest. Had this object exploded over a city, the consequences would have been fatal – the covered area is larger than e.g. the city area of Munich, Germany. An object of this size is expected to enter the Earth’s atmosphere statistically every few hundred years.

The number of known NEOs is increasing constantly. In 2024, the number of 35000 NEOs was reached. About 900 of them² are larger than 1 km and it is estimated that the total population for this size range is around 950, i.e. about 95 % are known (Granvik *et al.* 2018). A subset of the NEOs is called ‘Potentially Hazardous Objects (PHO)’ – these must have an orbital intersection distance with the Earth of less than 0.05 au or 7.5 Mio km and a size of larger than ~140 m. About 1300 PHOs are known at the time of writing. I try to avoid using this term, as objects smaller than 140 m can also be hazardous. In ESA’s Planetary Defence Office, the term ‘threatening object’ is used. This encompasses *all* objects that potentially could hit the Earth, independent of their size. For their number, check the web page of ESA’s Planetary Defence Office at <https://neo.ssa.esa.int>. They are listed as ‘NEAs in risk list’ on the title page. An independent determination of the risk list is performed by NASA’s JPL ‘Center for NEO studies’ (CNEOS), see <https://cneos.jpl.nasa.gov>.

The expected number density of objects grows exponentially as the size decreases – decreasing the size by a factor of 2 will result in an increase of number by a factor of about 3. For objects about the size of the Tunguska impactor (40 to 50 m diameter) we currently estimate that we know only 2 %.

¹ 1 au (astronomical unit) is the average distance between the Earth and the Sun.

² For the currently known number see <http://www.minorplanetcenter.org/>

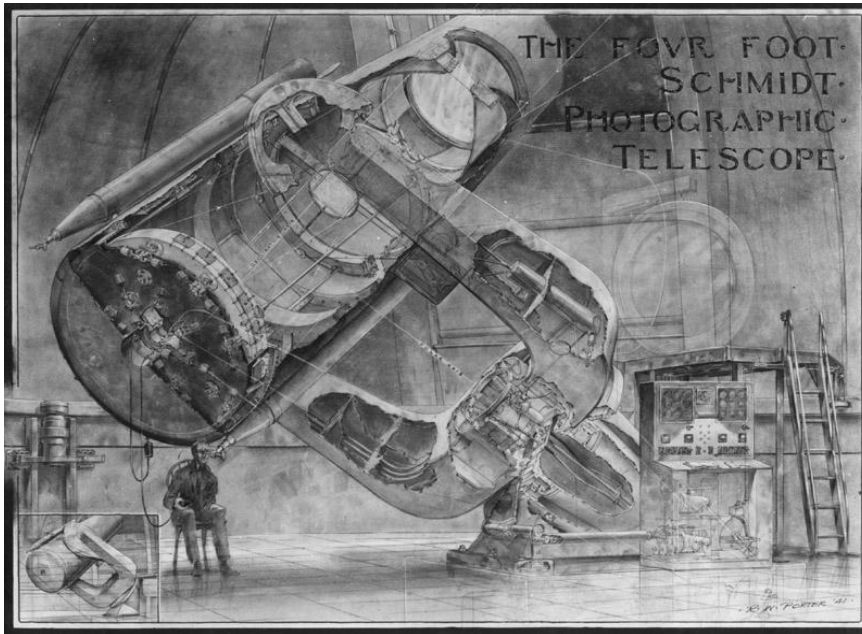


Figure 1: 48" Palomar Schmidt telescope (https://naturalimagesgallery.com/space_sky/palomar/four_foot_schmidt.jpg).

4. Where do asteroids come from?

Current scientific models assume that the solar system has formed about 4.6 billion years ago (e.g. Pflanzner *et al.* 2015). Figure 2 shows a sketch of the event. Suns and planetary systems are assumed to form in gas clouds such as the Orion nebula (Figure 3). The Hubble Space Telescope has discovered areas in this and other nebulae that are assumed to be proto-planetary disks, called 'proplyd' (Figure 4, O'Dell *et al.* 1993). Proplyds form when part of the gas cloud becomes gravitationally unstable and starts contracting. Upon contraction, the cloud starts spinning. Solid particles form and grow around the protosun in the centre. Once these solid particles have reached a size of meters to hundreds of meters, they are called planetesimals. Low-velocity collisions between the planetesimals allow them to grow, eventually resulting in the planets. As a starting point for further understanding this process, use Jansson *et al.* (2017) and the references given therein.

Not all planetesimals contributed to the formation of the planets. A large number of them are left in the solar system and undergo further collisional processing, resulting in the current asteroid and comet population (Koschny *et al.* 2019). For scientists this makes these objects very interesting – analyzing the oldest asteroids and comets allows the scientists to peek back into the past and constrain the formation of our solar system and ultimately the Earth.

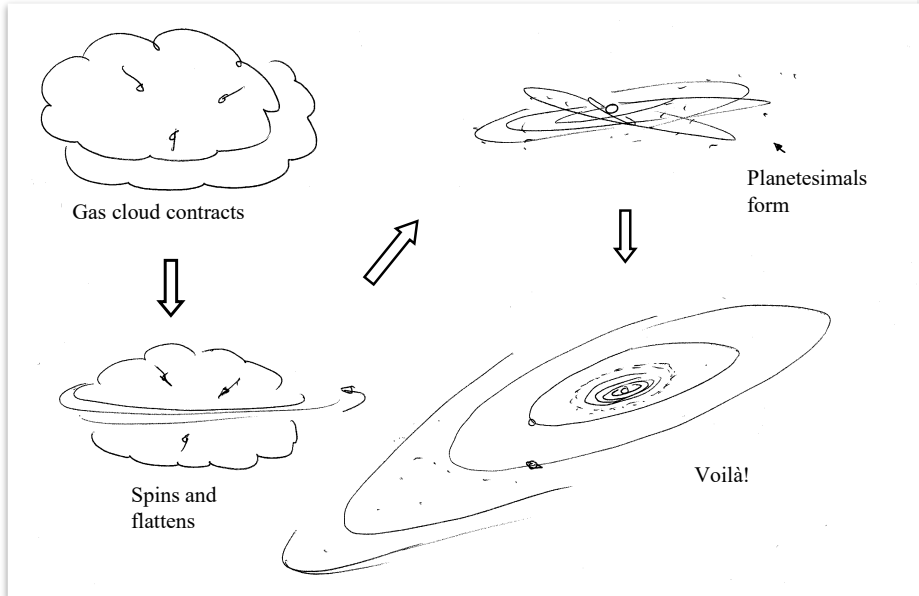


Figure 2: Sketch of the formation of the solar system.

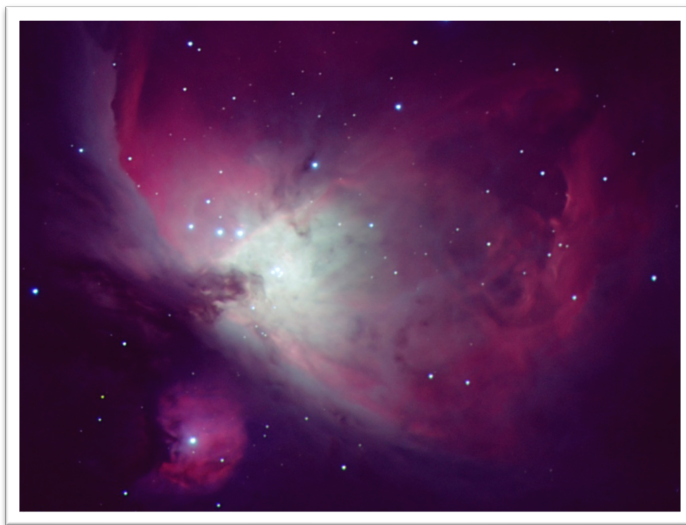


Figure 3: Amateur photograph of the Orion nebula. Image credit: R. Apitzsch, with kind permission.



Figure 4: A planetary system in the making - so-called 'proplyds' (protoplanetary disks) in the Orion nebula. Image credit: C.R. O'Dell (Rice University), and NASA.

Initially, most of the asteroids were in nearly circular orbits around the Sun. Dynamical modeling has shown that due to resonances with the large planets, in particular Jupiter, objects are deflected onto orbits with high ellipticity (see the later section on the ν_6 resonance). Due to non-gravitational effects, these resonance locations are always refilled with new objects, so the source will not deplete quickly.

Part of the objects will be sent away from the Sun, others will get closer to the Sun. This can bring them in the vicinity of the Earth. Thus, asteroids are not only of high interest to scientists who want to understand the formation of the solar system, but they also might be a threat to the Earth and our human assets. How to deal with this second topic is the focus of this script.

5. Terminology

5.1 Asteroids and comets

An asteroid is a small solar system body sized from almost 1000 km down to 1 meter. It is typically made up of rocky material and/or iron. In ground-based observations using telescopes, asteroids appear as small dots like stars (thus the name: asteroids = 'like a star'). If the object shows a coma around it, it is called a comet. Comets contain volatile material (ices) that outgas and form a tenuous atmosphere around the object (Figure 5).

If the object is so large that its gravity influences its environment significantly, it is called a planet. Objects which are smaller



Figure 5: Comet Hale-Bopp, a bright comet visible to the naked eye in 1997. The blue plasma tail is blown away by the Solar wind in the anti-Sun direction. The reddish-white dust tail roughly follows the path of the comet in space.

than asteroids are called meteoroids. The boundary has only recently been defined: An object smaller than 1 m is called meteoroid, one larger than that is an asteroid (Koschny *et al.* 2017). It should be noted that the Minor Planet Center would give out an asteroid designation even for objects which turn out to be smaller than 1 m, as long as they were discovered in space.

5.2 Main-belt objects

Most asteroids are located in a region between Mars and Jupiter, orbiting the Sun with a typical semi-major axis of about 2.2 to 3.3 au. They normally stay close to the ecliptic, with most objects having inclinations below 30°. These are called ‘main-belt asteroids’ (MBA). A small number of objects have been shown to have activity, i.e. they are outgassing volatile material. An outgassing object is normally called a comet and these objects are called ‘main-belt comet’. The combination of both classes is referred to as main-belt objects (MBOs).

The largest main-belt object is (1) Ceres with 950 km diameter. Most objects are only a few kilometers in size. Objects as small as a few tens to hundreds of meters are expected in the main belt. However, they are too faint to be observable from the Earth with our current instrumentation.

A few MBOs have been visited by spacecraft during flybys. The only MBOs that have ever been orbited by a spacecraft are (1) Ceres and (2) Vesta, which have been orbited by the US spacecraft Dawn in 2011-2012 (Vesta) and 2014-2018 (Ceres).

Commented [DK1]: Add references.

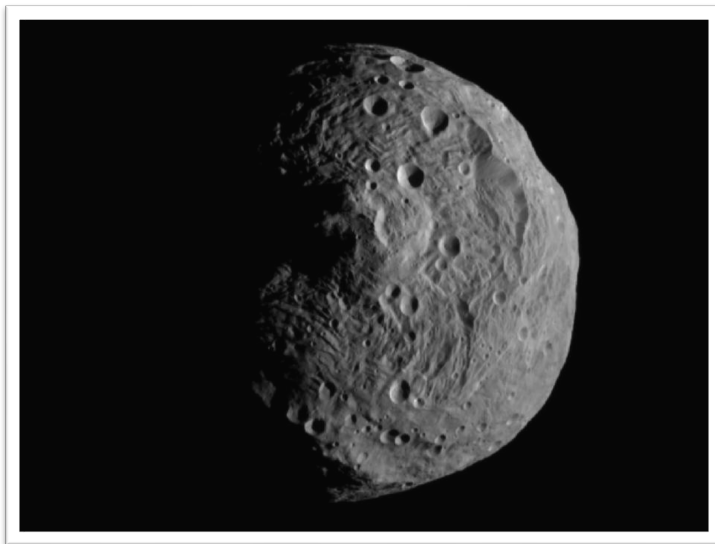


Figure 6: Image of the 530 km diameter asteroid Vesta, taken by the DAWN spacecraft with the German imaging system. Credit: NASA/JPL-Caltech/UCLA/MPS/DLR/IDA.

5.3 Near-Earth objects

The International Astronomical Union (IAU) has defined a near-Earth object (NEO – speak ‘en-ee-oh’) as an asteroid or comet with a perihelion of less than 1.3 au.

An example for an NEO is asteroid (433) Eros, which was visited by the US spacecraft NEAR-Shoemaker in the year 2000. NEAR-Shoemaker spent over a year orbiting the object. Figure 7 shows the asteroid as imaged by the spacecraft. The size of the object is 40 x 15 x 14 km³ in size and rotates about its axis once in about 6 hours.

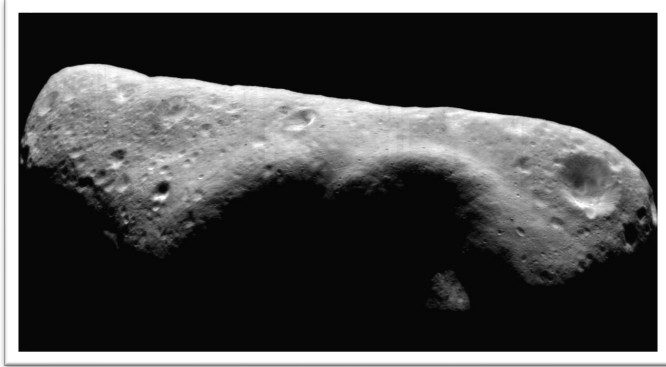


Figure 7: Asteroid 433 Eros as imaged by the NEAR-Shoemaker spacecraft. Credit: NASA/JHU.

5.4 Atens, Apollos, Amors, Atiras

NEOs are classified in four different groups named after the first object discovered that belongs to that group. These groups are linked to the orbital elements, in particular the apo- or pericentre distance and the eccentricity.

Amor asteroids are on an orbit that is close to the Earth, but never crosses the Earth's orbit. The perihelion is larger or equal than 1.02 au, which is the aphelion of the Earth's orbit. Their perihelion is less than 1.3 au; otherwise they would not fulfill the condition for an NEO.

Apollo asteroids also cross the Earth's orbit, but they have an orbital period larger than 1 year. Their semi-major axis is thus larger or equal than 1.0 au, and their perihelion smaller or equal 1.02 au.

Aten asteroids have a semi-major axis smaller than 1.0 au and an aphelion larger than 0.983 au (the perihelion of the Earth). Thus they do cross the Earth's orbit. Their small semi-major axis means that their orbital period is less than 1 year.

Atiras, (also called Inner-Earth Orbit (IEO) objects) always stay inside the Earth's orbit; they have an aphelion of less than 0.983 au. Thus they never cross the Earth's orbit, even at the closest distance of the Earth's orbit to the Sun.

Figure 8 summarizes this information in a graphical form.

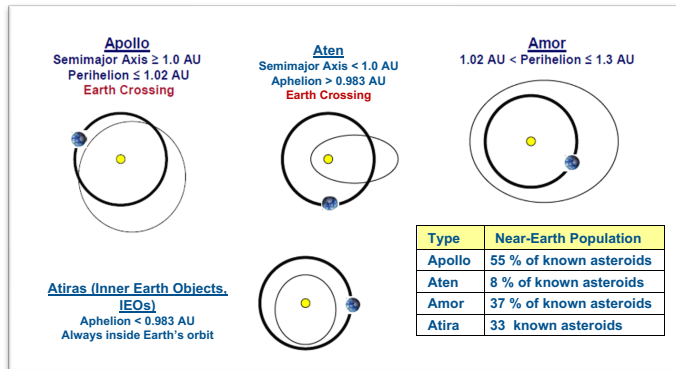


Figure 8: NEO families. Image credit: NASA 2007. The numbers of objects or percentages were obtained on 02 Jan 2024 using the 'advanced search' at <http://neo.ssa.esa.int/search-for-asteroids>.

5.5 Mean Orbital Intersection Distance

The Mean Orbital Intersection Distance (MOID) is the shortest distance between two orbits. Thus, it is the closest distance two objects can possibly have. However, at any given close encounter the actual distance between the objects can be larger, as the timing of the close flyby needs to be such that both objects actually are at the points where the MOID intersects their orbits.

5.6 Magnitude

The *magnitude* is a measure of brightness for objects in the night sky. Hipparchos divided the brightness of stars in six 'equal' classes from 1 to 6, '1' being the brightest stars. Since the response of the eye is non-linear, it turns out that objects with flux density relations of 1:10:100 look like having the same brightness difference (The flux density is the number of photons per second arriving in our eye).

From this, Pogson defined in 1856 the magnitude in a mathematical way. He noted that the brightness difference of 1 mag and 6 mag stars is roughly 100. He thus divided the ratio of the brightness of class n and class $n + 1$ to be the fifth root of 100, i.e. $100^{1/5}$, or ~ 2.512 .

If F is defined as the *flux density* in W/m^2 , then we can write

$$m - m_0 = -2.5 \log \frac{F}{F_0} \tag{1}$$

where F_0 is the flux density of a reference object, F the flux density coming from the object, m the magnitude of the object.

Note that in this formula, the constant 2.5 is precise, even though the magnitude difference is 2.512 – we leave it up to the reader to prove this.

The star Vega (alpha Lyra) has been defined as the reference star with the magnitude 0. For comparison, the Sun has a total magnitude of roughly -27.0 mag as seen from the Earth. A convenient way to convert flux densities to magnitude is by using the Sun as a reference, knowing that the 'solar constant', i.e. the flux density just outside the

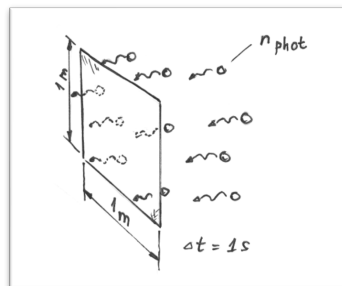


Figure 9: Visualizing the flux density.

Earth's atmosphere is $F_{Earth} = 1362 \text{ W/m}^2$. How to do this is described in Section 8.2.

Note that we have used the term 'flux density'. The unit is W/m^2 , or energy per time and area. This can be visualized as the number of photons passing through an area element of 1 m^2 in 1 s of time, see Figure 9. Each photon would carry the energy

$$E_{phot} = \frac{hc}{\lambda} \tag{2.}$$

Where h the Planck constant and c the speed of light ($h = 6.62606957 \cdot 10^{-34} \text{ Js}$; $c = 3 \cdot 10^8 \text{ m/s}$).

Increasing the number of photons results in an increase of the flux density. I.e. the brighter the illumination source, the higher. Note that from the above formula we can see that reducing the wavelength (i.e. an increase in the frequency) of the incoming light has the same effect. Thus, for precise computations the wavelength of the light has to be considered. A typically used standard wavelength range is the 'V' filter as defined in the following section.

5.7 Johnson-Cousins filter bands

The apparent magnitude of an object is dependent on the instrument used to determine it. Sensors are typically only sensitive in certain wavelength ranges. Comparing stars of different magnitudes that have different colors would give different results, depending on the spectral sensitivity of the sensor. To be able to correct for this, different authors have used different filter standards. In current astronomical research, the so-called Johnson-Cousins UBVRI system is widely used. It defines five standard filters in the UV ('U'), the blue ('B'), the visual range ('V'), the red ('R'), and the infrared ('I'). Figure 10 shows the definition of these filter ranges in a graphical way.

These filter standards were proposed by Johnson and Morgan (1953) and expanded by Cousins (1976).

The magnitude of the Sun is for example $M_{Sun, V} = -26.8$, $M_{Sun, R} = -27.1$.

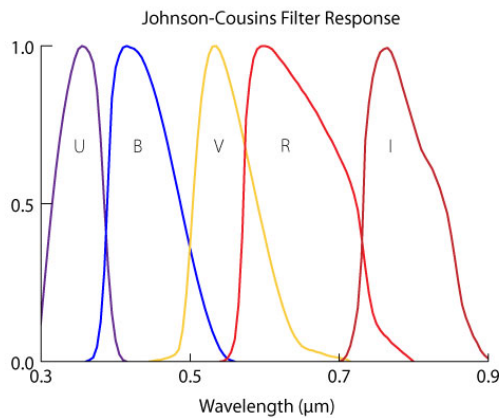


Figure 10: Transmission bands of the Johnson-Cousins filters U, B, V, R, I. Credit: <http://www.astrophysicspectator.com/topics/observation/MagnitudesAndColors.html#notetwo>.

Table 1: Filter ranges and average wavelengths for the UBVRI system.

Name	passband in nm	average wavelength in nm
U – ultraviolet	300 – 400	360
B – blue	360 – 550	440
V – visual	480 – 680	550
R – red	530 – 950	700
I – infrared	700 – 1200	880

5.8 Absolute magnitude

The *absolute magnitude* is the apparent magnitude of an asteroid or comet as seen from a distance of 1 au³, with the asteroid being 1 au from the Sun. Obviously it is not possible to realize this - it would mean that the observer is located on or actually in the Sun. Anyway, that is the definition.

Note that stellar astronomers use the absolute magnitude as the magnitude of a star as seen from one Parsec or 3.262 light years distance. Do *not* use that definition for asteroids.

5.9 Albedo

The albedo is the percentage of light that a surface reflects. Typical asteroid albedos are between 3.5 % and 40 %. For comparison: The Moon has an average albedo of 12 %. Snow reflects 90 % of the incoming light, charcoal about 4 %.

In particular for the dust and gravel layer covering most asteroids as well as the Moon, the albedo strongly depends on the direction of the incoming light and the viewing direction. Strictly, the average albedo over all wavelengths and over all phase angles is called bond albedo (after the US astronomer Bond, 1825 – 1865). In the text here we simplify the terminology and always just use the word albedo.

5.10 Potentially Hazardous Objects

A Potentially Hazardous Object (PHO) is an asteroid or comet with a MOID of less than 0.05 au (ca. 7.5 Mio km) and an absolute magnitude brighter than 22. This magnitude corresponds to about 140 m diameter for an object with 14 % albedo.

Note that this seems to imply that an object smaller than 140 m is not hazardous anymore. The authors disagree – and have introduced the term ‘threatening object’. A threatening object is any object which may impact the Earth. Even at 2 m size, it may produce a bright fireball which merits notification if predicted. A bright fireball may *e.g.* be mistaken with a missile attack and could thus be threatening.

5.11 Asteroid families

Asteroids are also classified in ‘families’. The definition of the families is linked to their orbital parameters and therefore – most likely – their evolutionary history. Figure 11 shows a diagram of inclination versus semi-major axis of all asteroids. In this diagram, clumps of objects can be seen. They are separated in semi-major axis by the so-called Kirkwood gaps. These are cleaned out of objects by resonances, mainly with Jupiter.

Asteroid families are normally named after the largest object in this orbit. Asteroids belonging to one family may originate from the same parent object, possibly generated when a large impact destroyed the parent.

³ 1 au is the average distance between the Earth and the Sun, 1 au = 149.6 Mio km. Note that since 2013, the IAU has defined ‘au’ to be spelled with small letters.

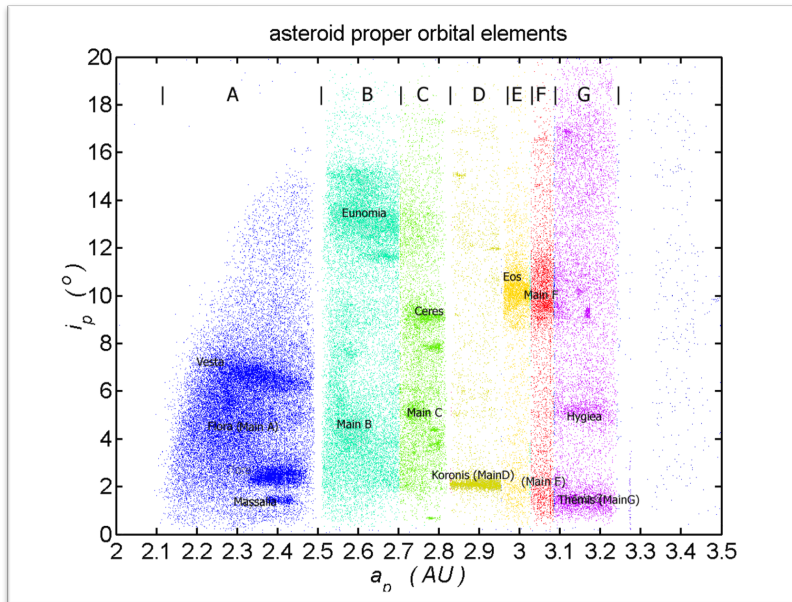


Figure 11: Inclination versus semi-major axis for all asteroids. The text indicates asteroid families. The so-called Kirkwood gaps are clearly visible. These are resonance areas in which asteroids can not reside for a longer period of time. The Kirkwood gaps divide the asteroid population in the areas called A to G. For a real-time version of this diagram, see <http://www.minorplanetcenter.net/iau/plot/OrbEls51.gif>.

5.12 Nu6 resonance

The nu6 (ν_6) resonance, together with a 3:1 mean motion resonance with Jupiter, is the main source for NEOs. It is a resonance that is linked to some properties of the orbit of Saturn (thus the index '6', Saturn is the sixth planet counted from the Sun). It works like this:

Since asteroids as well as planets move in a gravitationally perturbed environment, the longitude of perihelion of their orbit, which would be constant in the 2-body problem, is not really constant but moves over time. This movement – called precession - is a function of both the orbital semi-major axis and inclination. Simplified, the nu6 resonance occurs when the asteroid's longitude of perihelion precesses with the same frequency as that of Saturn (strictly speaking it is a bit more complicated, but this explanation is close enough). It can be shown semi-analytically and by numerical integration that if an asteroid gets into this resonance, its eccentricity increases very quickly while the semi-major axis remains constant. For a given semi-major axis, the increase of the eccentricity decreases the perihelion distance (minimum distance to the Sun), and therefore this will bring the asteroid's orbit close to the Earth. Typically, the time it takes for an asteroid in the main belt to be transported to the Earth-crossing region is of the order of a million years by this resonance.

This resonance is called a secular resonance, because the rate of precession of the orbital angles is very slow (tens to hundred thousands of years to make one cycle), contrary to mean motion resonances which involve the orbital period, which is much shorter (1 year at the Earth's semi-major axis, 11.9 years at Jupiter's semi-major axis)(Michel 2012, pers. comm.).

In Figure 11, the nu6 resonance produces the cut-off on the left side of the Vesta and Flora families, starting at around 2.1 au and 0° inclination to 2.4 au and 15° inclination.

5.13 Observatory code

All observatories world-wide that measure positional (astrometric) data of asteroids provide them to the central clearing house, the Minor Planet Center (MPC⁴). To identify the observatory, they must have a so-called *observatory code*. To obtain such a code, an observatory must send astrometric measurements of at least two main-belt asteroids from at least two nights. The MPC then applies some checking algorithms to see whether the data quality fulfills the requirements. If yes, a code is awarded.

The codes are three-digit numbers or a letter and two numbers. An example: ESA's 1-m telescope on Tenerife, the 'Optical Ground Station', has the code J04. The private observatory of the author in the Netherlands has the code B12.

The code is uniquely linked to a location on the Earth with fixed geographical coordinates and elevation above zero. It is also linked to a fixed name. Many websites related to asteroid observations allow entering the observatory code and from that know the location of the observatory.

Since the MPC is working under the auspices of the IAU, often the term 'IAU observatory code' is used.

5.14 Conjunction, elongation, and opposition

As we will see later, planets and asteroids orbit the Sun in elliptical orbits. To describe special positions in the relative location of an asteroid or planet relative to the Earth, the following terms are used:

- Opposition: The asteroid or planet is in the opposite direction relative to the Sun.
- Inferior conjunction: The asteroid or planet is exactly between the Sun and the Earth.
- Superior conjunction: The asteroid or planet is behind the Sun as seen from the Earth.

Note that these terms can also be used relative to other objects than the Earth.

6. From observations to measurements – the current state of near-Earth object observations

This section gives a short overview of the way asteroids are found and observed, how the data flows to the different processing centers, and how the results are distributed and fed back into the planning process. Later sections focus on some of the steps below in more detail.

The process of finding new NEOs involves several players:

- (a) Survey telescopes which scan the night sky;
- (b) The Minor Planet Center (MPC) which collects positional measurements ('astrometry') of all asteroid observers worldwide; it computes a preliminary orbit of newly detected objects and announces these on a so-called 'NEO Confirmation Page';
- (c) Follow-up observers which take this information and attempt to re-observe the objects at a later point in time;

⁴ MPC = Minor Planet Center (<http://www.minorplanetcenter.org/>)

- (d) The MPC now can compute a better orbit. If the object is a new NEO, it announces it in a so-called Minor Planet Electronic Circular (MPEC);
- (e) Two separate data processing centers – the Sentry system at JPL and the NEODyS⁵ system at the University of Pisa compute high-precision orbits with these data, propagate the orbit into the future, and compute closest distances to the Earth;
- (f) In case of a possible impact, NASA has a procedure in place to warn the relevant authorities via diplomatic channels; ESA is currently working on such a procedure;
- (g) If an asteroid deflection were necessary, this could be technically feasible already today. The decision process for such a mission is currently being discussed within a UN-endorsed group called Space Mission Planning Advisory Group (SMPAG⁶).



Figure 12: One of the telescope domes of now discontinued the La Sagra Sky Survey in Southern Spain.

In this section more details for steps 1 to 5 are given. Steps 6 and 7 are discussed in a separate section.

Several survey telescopes on this planet scan the sky every clear night. The telescopes are operated such that they scan a small part of the sky repeatedly to image the same sky field 3-5 times in time intervals of several minutes to half an hour. An asteroid becomes visible in these image sequences as a dot moving in a straight line.

Automated detection software can identify these objects. The software also determines the precise plate solution of the image, i.e. the pointing positions and optical distortions. From this information, the position in celestial coordinates of the moving object can be automatically determined.

If the position matches the expected position of a known asteroid, the position measurements can be attached to the designation of that object. If the position does not match a known object, it is flagged as a potential new discovery and given a temporary designation by the observer (a typical temporary designation could be OGS2292). To ensure the data quality and avoid false detections due to noise some surveys involve a human operator who visually inspects thumbnail images of the potential detections and confirms or rejects the detection.

All measured position information is sent to the Minor Planet Center (MPC). This is true not only for survey observatories, but for all observatories measuring asteroid or comet positions. The MPC is located in Massachusetts, USA. It was mandated by the International Astronomical Union as the one place in the world to collect asteroid position data, identify new objects, and give unique designations to asteroids.

When receiving position measurements of newly observed objects the MPC runs computer software to match the positions to existing objects (called 'linking'). If no matches are found, it is a possible new object. The software estimates a probability for the object to be an NEO. If this probability is non-zero, the object is posted on the NEO Confirmation Page (NEOCP) of the MPC.

This page allows other observers to compute the apparent position of the object in the sky from their observatory. They then point their telescope to this position and attempt a so-called 'follow-up'

⁵ NEODyS = Near-Earth objects Dynamics Site (<http://newton.dm.unipi.it/neodyS/index.php?pc=0>)

⁶ SMPAG = Space Mission Planning Advisory Group

observation. If successful, they also submit their observations to the MPC. Once enough observations for a given object have been sent in to allow either a positive confirmation or a rejection of an NEO, the object is announced in a Minor Planet Electronic Circular (MPEC). The object is taken off the NEOCP; the MPEC assigns it an official provisional designation. A typical designation is 2011AA – this would be the first object discovered in the first 2 weeks of 2011.

Only after the object has been observed after two or three well-observed oppositions it will receive a final number (e.g. 21686). Then, the discoverer has the right to give a name to the asteroid. He/she cannot name the asteroid after him/herself, but any other reasonable name will normally be acceptable.

Once an object has been announced in an MPEC, the position measurements related to it are used by two independent data centers for more precise orbit calculations. One is the so-called Sentry system at JPL, one is the European ‘NEO Dynamics Site’ (NEODYs) of the University of Pisa. NEODYs has been federated into ESA’s NEO segment and can be reached via the ESA web pages⁷.

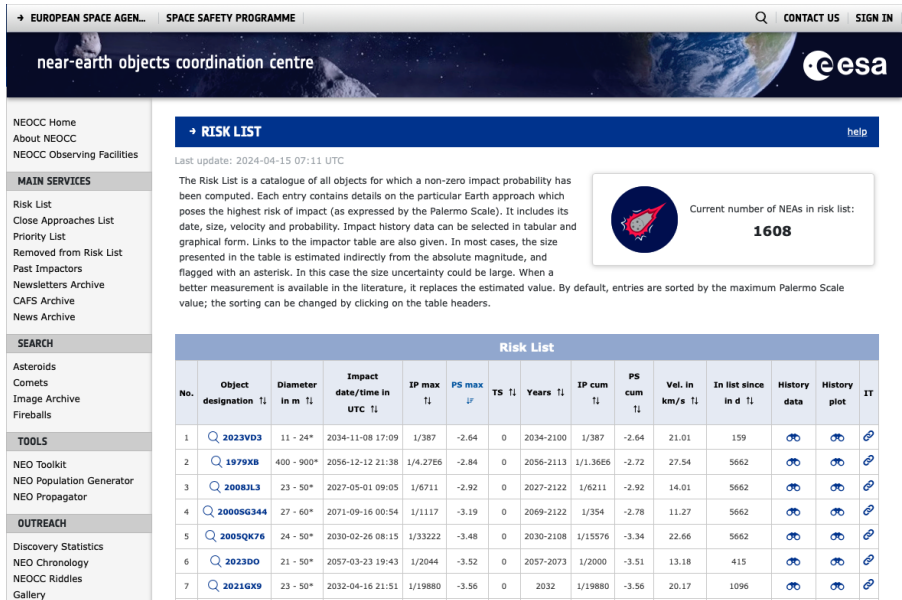


Figure 13: The risk by ESA, showing the objects with the highest risk of impacting the Earth.

These centers perform high-accuracy orbit computations and in particular propagate the orbit into the future to find possible close Earth flybys. They take the perturbations of the main planets (in particular close flybys at the Earth) into account. Due to the errors in the observational data, the orbit cannot be precisely predicted. NEODYs thus computes orbits for several thousand ‘virtual impactors’, which have slightly different starting conditions compared to the average observed orbit. These virtual impactors are all propagated 100 years into the future and from that a probability of impact with the Earth is computed.

The ultimate result of the process is called the ‘risk list’. It gives a list of objects with a non-zero chance of hitting the Earth with their absolute magnitude (a measure of their size) and information on when they could be observed again. For each object, a table with the upcoming close Earth flybys and the respective probabilities of hitting the Earth are given.

⁷ <http://neo.ssa.esa.int/risk-page>

In 2013, there were somewhat over 400 objects in the risk list; object 2007 VK₁₈₄ has the highest chance of hitting the Earth. The object has an estimated size of 150 – 200 m. It has a chance of a bit less than 0.1 % of the background impact risk to hit the Earth on 03 Jun 2048. If it were to hit the Earth, an object of several tens of meters would most likely reach the ground and generate at least regional damage. In 2024, the number of objects has increased to about 1600. This is due to a better computational system, and to the increased number of objects in general.

7. Ongoing ground-based survey programs

The regular search for NEOs on a large scale began less than 20 years ago, most of them in the USA. A congressional directive to NASA to conduct such a program was given in 1998. The directive states that 90 % of all NEOs larger than 1 km should be identified within 15 years.

As mentioned in the previous section, the currently most successful asteroid surveys are the NASA-funded Catalina sky survey and Pan-STARRS. In Europe, the now defunct La Sagra Sky Survey (LSSS), an amateur program, deserves mentioning. ESA is testing survey strategies in a program called Teide Observatory Tenerife Asteroid Survey (TOTAS).

The following sections give more details on recent ground-based NEO survey programmes. Space-based programmes (like the NEOWISE project) are not (yet) discussed in this text.

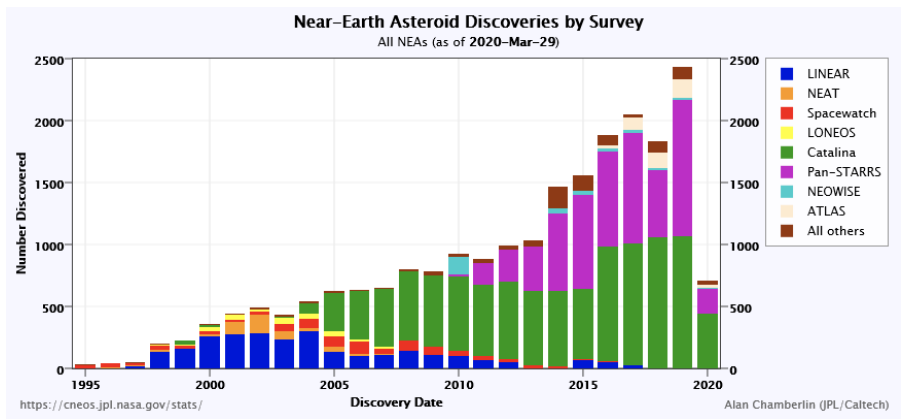


Figure 14: NEO discoveries as a function of time and survey program. Download the latest version from https://cneos.jpl.nasa.gov/stats/site_all.html.

Figure 14 shows the NEO discoveries since 1995 in half-year intervals. It can be seen that the survey program started with Spacewatch. Very quickly the military-funded LINEAR program became successful. Around 2004 the Catalina sky survey became the most successful survey program, now Pan-STARRS is the most successful one.

In this Chapter we will look at these surveys in a bit more detail.

7.1 Catalina Sky Survey

The Catalina Sky Survey (CSS)⁸ has been the most successful NEO survey between 2005 and 2014. This sky survey uses several old telescopes which have been refurbished with new electronic CCD cameras. It uses a number of telescopes:

- A 68/76 cm f/1.9 Schmidt telescope (the first two numbers refer to the diameter of the corrector plate and the main mirror; f/1.9 means that the focal length is 1.9 times larger than the diameter of the main mirror). This telescope is located on Mount Bigelow, north of Tucson in Arizona, USA (IAU code 703).
- A 50 cm Schmidt telescope in Siding Spring, Australia. This telescope was used for survey activities (IAU code E12) but stopped operations in 2013.
- A 1-m telescope for follow-up observations was used from Siding Spring in Australia typically 5 nights per month but stopped operations in 2013.
- A 1.5 m f/2 telescope on Mt. Lemmon in the USA (IAU code G96).

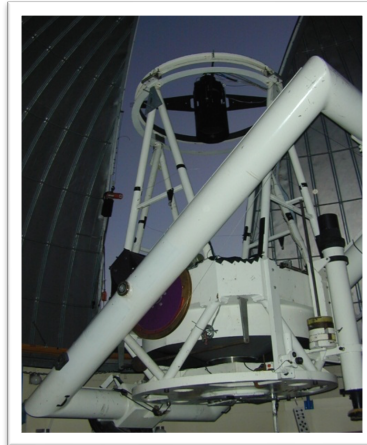


Figure 15: One of the Catalina Sky Survey telescopes. Credit: CSS.

7.2 Pan-STARRS

Pan-STARRS started operations in 2010. The acronym stands for Panoramic Survey Telescope & Rapid Response System. In the final stage, it will consist of four 1.8 m telescopes. Currently, two of these instruments are in operation at the observatory of Hawaii. Pan-STARRS has a very large CCD camera with 1.4 billion pixels, covering a field of view with a diameter of 3°. The telescope constantly scans the sky, covering the complete sky three times in the dark times of a lunar cycle.

While reducing the NEO threat is currently the primary goal of the telescope, until 2013 it also covered other science areas. It allows finding asteroids in general, for example Kuiper-Belt Objects which are not yet well known. It was also used for the search of exoplanets and scientific measurements addressing stellar and galactic evolution. In spring 2014 the project finished its initial survey and Pan-STARRS is currently funded 100 % by NASA's NEO programme.

7.3 La Sagra Sky Survey

The now discontinued La Sagra Sky Survey (LSSS) has been developed purely by amateur astronomers. Starting on the island of Mallorca, they used support from the regional government to set up an observatory, the Observatorio Astronomico de Mallorca. The main goal of the observatory was education, but from the beginning they wanted to perform also scientific work. As the sky conditions on Mallorca are suffering from more and more light pollution, they moved the scientific part of their observatory in 2004 close to the mountain La Sagra, next to the small village Puebla de Don Fadrique, in the south of Spain. There they had operated three 45-cm f/2.8 telescopes. With 16 NEO discoveries in 2011 it was number seven in the ranking of discoveries, preceded only by the large US survey programs. The IAU

⁸ <http://www.lpl.arizona.edu/css/>

code of the LSSS is J75. In 2014, the sky survey stopped its work from that location. Partially with the help of the company Deimos, the telescopes have been deployed in other locations.

7.4 Teide Observatory Tenerife Asteroid Survey

In 2009, two amateur astronomers used the 1-m telescope of ESA for one week to observe asteroids. One of them, M. Busch from Germany, had created a software to command the telescope in an asteroid survey mode. During their one week of observations they showed that this telescope can be successfully used for asteroid discoveries.

Starting in 2010, the NEO segment of ESA's Space Situational Awareness programme started using this telescope ca. 4 nights per month for asteroid observations. The main focus is on follow-up observations. But part of the night ESA is working together with M. Busch and operating the telescope in survey mode. The author was the initiator of this project from ESA side, therefore we will look at it in more detail to describe how a survey programme is performed.

The field of view of the telescope is about $0.7^\circ \times 0.7^\circ$. A sky area of $4^\circ \times 4^\circ$ is scanned by taking 25 images with an exposure time of 30 s. The telescope performs this scan 4 times after each other, thus obtaining four images about 15 min apart of the same sky area. An automated data processing pipeline finds stars in the images and matches them to a star catalogue. Objects which cannot be matched are noise, satellites, or asteroids. They are called *loners*. In the 15 minutes between images, a typical main belt asteroid will move between 15 and 30". With the camera settings we are using this corresponds to about 10 to 20 pixels. The software checks for all detected non-star objects whether they seem to be moving on a straight line. If yes, they are marked as a *'mover'*.

The positions of these movers are compared to the expected positions of known asteroids in the image. If these match, then the positions are marked with the designation of the known asteroid and stored. If they don't match, they correspond to a potential new object. 'Match' means:

- The mover must be closer than 40" (seconds of arc) to the catalogue object;
- The difference in apparent speed must be smaller than 0.1"/min;
- The different in apparent velocity direction (position angle) must be smaller than 3.5° .

Task 1: Take ESA's OGS (Optical Ground Station) telescope on Tenerife. The main mirror has 1 m in diameter. For asteroid observations, it is used in an f/4.4 configuration. The CCD camera used has a pixel size (see next section) of $d_{\text{pixel}} = 15 \mu\text{m}$. What is the image scale per pixel?

Thumbnails of the movers of these potential new objects are extracted and posted on a web site where they are inspected by a team of volunteers. These visually inspect the images and make a decision on whether the object is real or not. The automatically determined positions of all objects which were flagged as real are collected by the software. After a final check by M. Busch they are submitted as new discoveries to the MPC.

A screenshot of the checking interface for possible new objects is shown in Figure 16. This object has been confirmed in the meantime and has been given a name.

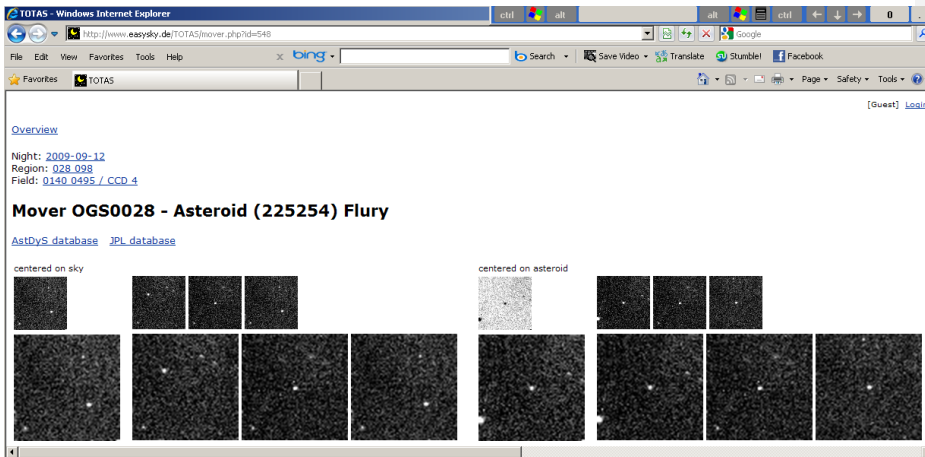


Figure 16: Screenshot of the TOTAS user interface. This is a screenshot of the first year of operation of the survey, where only three instead of four images were obtained.

8. Detection limits for asteroids

8.1 Introduction

In this section the basic equations to estimate the sensitivity of a telescope are derived.

The asteroid is illuminated by the Sun. Using the solar constant and with the distance of the asteroid to the Sun, we can compute the light energy which the asteroid receives in Watt or number of photons. The asteroid reflects a certain percentage of light – determined by the albedo. To estimate the light received by the telescope, the phase angle under which the asteroid is visible has to be taken into account.

The telescope will collect a certain light energy (number of photons) depending on its collecting area. It focusses an image on the detector where the asteroid is imaged as a point – or actually following a Gaussian distribution on the sensor due to diffraction in the optics.

The sensor – nowadays one uses CCD⁹ or CMOS¹⁰ cameras for this – converts photons in electrons. The sensitivity is described by the so-called Quantum Efficiency (QE), which is the percentage of photons which are converted. Typical numbers are $QE \sim 0.8$ in the visible wavelength range. These electrons are read out and converted to ‘Digital Numbers’ (DN) which can then be used in a computer to display the image.

In the following sections the three steps are described in more detail.

8.2 Brightness of the asteroid

An easy way of computing the brightness of an asteroid is to compare the flux it receives with that of the Sun at 1 AU (i.e. at the Earth) and noting that the magnitude in the standard V-filter (V = visual, centered around 550 nm) is $M_{Sun} = -26.8$. Remember from Section 5.6 that the solar flux density F_{Earth} at the Earth is 1362 W/m^2 or roughly 1.4 kW/m^2 .

⁹ CCD = Charged-Coupled Device

¹⁰ CMOS = Complemental Metal-Oxide Semiconductor

The flux density reduces with the square of the distance. The flux density at the asteroid can be computed with

$$\frac{F_{ast}}{F_{Earth}} = \left(\frac{1AU}{r_{ast}}\right)^2 \quad (3.)$$

with r_{ast} the distance between asteroid and Sun in au.

With the albedo p of the asteroid and distance asteroid – Earth being d_{ast} , the flux arriving at the Earth is:

$$\frac{F_{ast,Earth}}{F_{ast}} = \frac{1}{4\pi d_{ast}^2} p A f(\varphi) \quad (4.)$$

φ is the angle between Sun and Earth as seen from the asteroid. $f(\varphi)$ is the phase function of the asteroid, A the area of the asteroid. The factor $1/4\pi d_{ast}^2$ can be explained as follows: Assume one square meter of asteroid surface is illuminated with n photons. If they are homogeneously scattered, they will be distributed over the complete half sphere above the surface. If the observer is at a distance of d , the given factor describes the reduction in photon density.

The proper phase function is a complicated combination of illumination conditions and asteroid surface properties. For the simple estimate here, a spherical object which homogeneously scatters light in all directions (Lambertian scatterer) is assumed. Then, $f(\varphi)$ reduces to:

$$f(\varphi) = \frac{1}{2}(1 + \cos(\varphi)) \quad (5.)$$

Again note that the real functional relation in use for asteroids is more complex and will be described in more detail in a future revision of this document. See *e.g.* Muinonen *et al.* (2010) for a much more accurate form of the formula above.

With these equations, we can compute the magnitude of an asteroid as seen from the Earth:

$$m_{ast} - M_{Sun} = -2.5 \log \left(\frac{F_{ast,Earth}}{F_{Sun,Earth}} \right) \quad (6.)$$

8.3 Telescope throughput

Telescopes collect light either via a mirror (reflector) or lens (refractor). Mirror systems can be built larger, as the mirror can be supported from the back. There are many different telescope types and configurations. These will not be discussed in detail here; rather, we assume a simplified telescope design consisting only of a main concave mirror and the sensor. Figure 17 shows a sketch of a typical reflector. The incoming flux density F is collected by the mirror with a surface area A . The mirror typically has a parabolic shape, focusing the image onto the sensor. To achieve a large field of view, the telescopes should have a small focal length. The so-called f-ratio (f_r) is defined as:

$$f_r = \frac{fl}{d} \quad (7.)$$

With fl the focal length of the telescope, d it's diameter. The f-ratio is often called 'f number'. An f-ratio of 4 is often written as 'The telescope is an $f/4$ telescope'. Typical wide-field telescopes are nowadays built with $f/6$ to $f/4$. f -ratios of 2.8 are available on the market nowadays. However, they require lens correctors before the sensor, which reduce the sensitivity dramatically in the UV and IR wavelength ranges. Because of absorption and scattering, they also reduce the sensitivity of the telescope in general.

One aspect of a telescope is the field of view and the pixel scale. The larger the focal length, the smaller the field of view for a given sensor size. The pixel scale sc can be computed by

$$sc = \arctan(d_{pixel} / fl) \quad (8.)$$

$$sc \approx d_{pixel} / fl$$

with sc in radians and d_{pixel} the size of one pixel. The pixel scale is typically given in arcsec/pixel, e.g. the OGS telescope of ESA has $sc = 0.66''/\text{pixel}$.

One can define the *throughput* τ of a telescope as the ratio of light arriving on the detector versus incoming light. Typical throughput values are $\tau \sim 0.8$ for the visible wavelength range for an all-mirror system. Using a field flattener – typically consisting of several lenses through which light has to pass – can reduce this value to ~ 0.6 .

To be able to mount the sensor in the focal plane of the mirror, one either mounts the camera directly in the incoming light path, or at the side of the telescope tube. Then the light needs to be directed out of the telescope tube via a mirror system. Thus the main mirror is obstructed, reducing the light collecting area. Typical obstruction values are 15 – 30 %.

Putting everything together, the flux arriving from the target on the detector can be written as:

$$F_{Detect} = F_{in} \cdot (A - A_{obstr}) \cdot \tau \quad (9.)$$

where F_{Detect} the detected energy per time, W, F_{in} the incoming flux density (energy per time per area, W/m^2) from the object, A the surface area of the prime mirror in m^2 , A_{obstr} the area of the obstruction in m^2 , and τ the throughput. A note to the units of F_{Detect} : The reader will have noticed that the 'per area' has gone in the units. While the same symbol (F) is used, this is now a energy per time, not a flux density any more. Visualize that all the light coming from a point-like object, collected by a telescope mirror with a certain area, is now concentrated in one point. Thus, no area dependency is there any more.

Due to diffraction effects, a star is not imaged into a real point. The light of a point source will be spread out to follow a Gaussian shape, see Figure 21. The size of the star in the focal plane is described by the *Full Width Half Maximum* (FWHM) of the Gaussian. The smaller the FWHM with respect to the pixel size, the more photons are collected in one pixel and the Signal-to-Noise (SNR) ratio of the star increases.

The fact that stars generate signal on more than one pixel can be used to improve the astrometric accuracy. Modern astrometry software measures the pixel values in an area around the star and determines the center position by finding the photometric center of the Gaussian. With this method, one can achieve measurement accuracies of down to 1/10 of a pixel.

The Gaussian shape of a star image in the focal plane is also affected by the *seeing*. The seeing is a measure of the turbulence in the air. It is expressed by describing the average FWHM of a star in arcseconds. At good astronomical sites, values of better than 1'' are reached. Typical values are 1.5'' to 2.5''. This often limits the SNR of the instrument more than the spread of the light by diffraction.

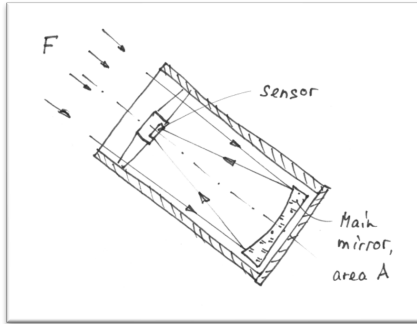
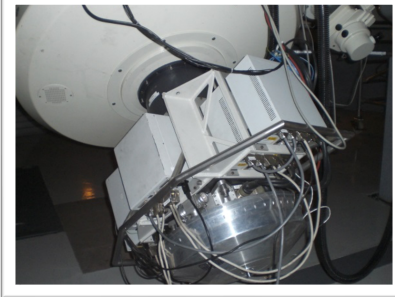


Figure 17: Sketch of a telescope (left) - incoming flux density F in W/m^2 , surface area A in m^2 . The area covered by the sensor (or often a secondary mirror) is called the obstruction. The right photograph shows the view into the tube of ESA's OGS telescope, giving an impression of the central obstruction.

8.4 Detection in a CCD camera

Nowadays basically all asteroid observations in the visible wavelength range are performed with a CCD camera. CCD stands for 'Charged-Coupled Device' and is the light-sensitive sensor in the camera. Additional elements of a CCD camera are a shutter, read-out electronics, and power supply.

A CCD consists of a specially doped silicon waver. It has a pixel structure that can be read out via a read-out register, see Figure 17. By opening a mechanical shutter, the exposure starts. Photons hitting the silicon generate electrons, which are trapped in the pixel and accumulate. The exposure ends when the shutter closes. Then CCD rows are 'clocked' into the readout register and read out one by one via a charge amplifier into a computer. The image is then represented by an array of bytes, with the value in one array element (called Digital Number, DN) being a function of the percentage of photons converted (Quantum Efficiency, QE) and the gain g of the charge amplifier.



Unfortunately, the QE of CCDs is a function of wavelength. This comes from the interaction of the photons with the silicon. For modern, so-called back-illuminated, devices, the QE can be as high as 80 % for the visible, dropping quickly in the dark blue to UV, and in the IR range.

Figure 18: The CCD camera of ESA's OGS telescope, used for NEO and space debris observations.

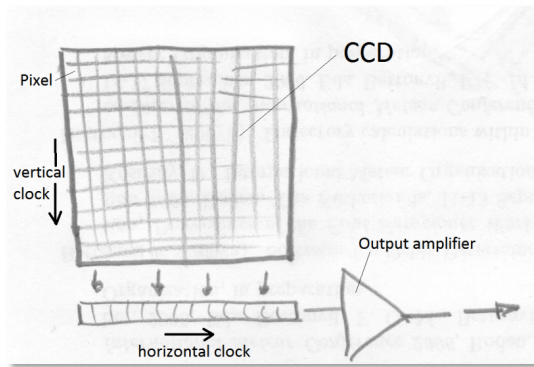


Figure 19: Sketch of a CCD detector.

Modern commercial CCD cameras typically have sensors with 1024×1024 pixel², 2048×2048 pixel², or even 4096×4096 pixel². Special cameras use mosaics of several sensors. The Pan-STARRS telescope uses a CCD camera with 64×64 many individual CCDs, each in turn consisting of 8×8 sensor areas with 600×600 pixel² each. Each 8×8 sensor has a physical size of about 5×5 cm².

Each pixel can only hold a certain number of electrons before it becomes saturated. This value number is called *full well (FW)*. Typical values are $FW \sim 80000$ to 200000 . Larger pixels allow larger full well. However, larger pixels mean lower spatial resolution for a given physical size of the field of view.

Typical pixel sizes are $9 \mu\text{m}$ to $13 \mu\text{m}$. With current technology, pixel sizes as small as $5 \mu\text{m}$ can be produced.

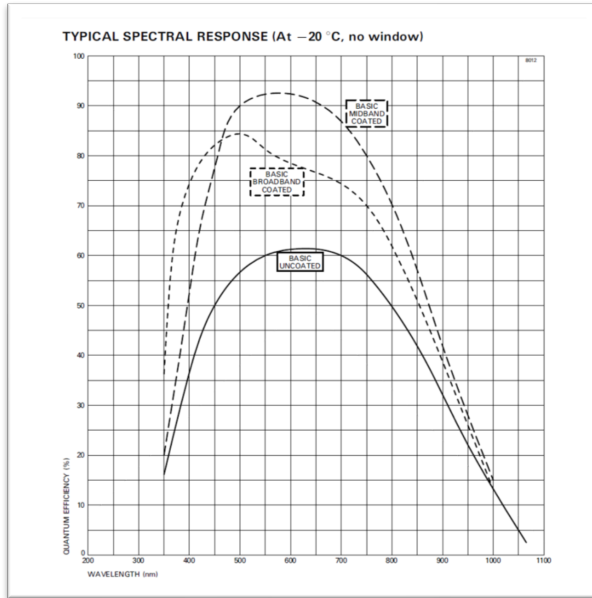


Figure 20: Quantum Efficiency of a CCD '42-40' from the company E2V. The three different curves denote different coating options, changing the spectral behavior of the response.

When used below the saturation limit, CCD sensors are linear. This makes them ideal for precise scientific measurements. The Digital Number of a pixel can be computed by

$$DN_{Signal} = t_{exp} \cdot p_{px} \cdot \frac{1}{g} \int \frac{F_{Detect,\lambda}}{hc/\lambda} QE_{\lambda} d\lambda \quad (10.)$$

where λ the wavelength, $F_{Detect,\lambda}$ the spectral flux density (the energy per time and wavelength arriving at the detector). Using λ as a subscript indicates that the spectral flux density and QE are a function of wavelength. The term hc/λ converts the spectral flux density in Wm^{-1} to number of photons, with h the Planck constant and c the speed of light ($h = 6.62606957 \cdot 10^{-34}$ J s; $c = 3 \cdot 10^8$ m/s) t_{exp} is the exposure time in seconds; p_{px} is the percentage of light on the center pixel.

g is the gain of the camera which is the conversion factor for the analog-to-digital converter of the camera electronics. It is characteristic of the camera and can be set by the manufacturer. It should be set such that the complete dynamical range is exploited. Assume the following: A video camera records a PAL signal, which has 256 grey levels (8 bit). The full well of the sensor is 50000 electrons. Here it would make sense to set the gain to $50000/256 = 195$ electrons/DN. The maximum number of electrons possible in one pixel – 50000 – would then be converted to the largest possible digital number, namely 255. For a professional CCD camera, typical full wells are 100000 e- and they are read out with 16 bit or $2^{16} = 65536$ grey levels. Here, a typical gain used would be 1.5 electrons/DN. The OGS telescope of ESA uses a camera with 0.9 e-/DN. Note that the term 'gain' is a bit misleading. It is a convention for camera manufacturers to use the unit e-/DN, which means one has to divide by the gain. This may be counterintuitive, but is the convention.

To explain p_{px} , consider Figure 19. Because of diffraction effects, the light from the star is distributed over several pixels. Typically, the camera/telescope combination is set up such that the full-width half maximum (FWHM) of a star is around 1.5 to 2 pixel, as shown in Figure 21 (right). In addition to the

quality of the telescope, the stability of the atmosphere (called 'seeing') is a major factor which determines the FWHM, and thus p_{px} . A typical value for p_{px} is 40 % or 0.4.

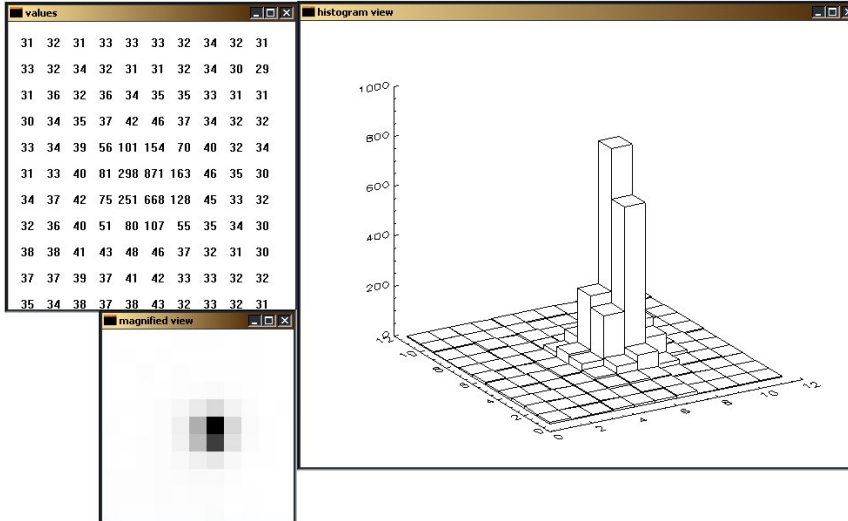


Figure 21: Zoom of a typical CCD image ('magnified view'). An inverse of the image is shown in the 'magnified view'. The upper left window shows the numbers which are in the actual image file and displayed by the computer as different brightness values. The numbers in each pixel are called Digital Number (DN). The right window shows a histogram view of the star. The light from the point-like star is distributed over a three-dimensional Gaussian shape.

To simplify (9), we remember that Johnson and Cousins have defined a convenient standard filter system. In the following we assume that all fluxes are corresponding to a flux in the R filter. QE then corresponds to an average Quantum Efficiency in the R filter band. For example for the E2V CCD 42-40, the average QE in the range 530 nm to 950 nm, centered around 700 nm, can be taken from Figure 20 to be roughly 80 % or 0.8 for a mid-band coated sensor.

Then (9) simplifies to

$$DN_{Signal} \approx t_{exp} \cdot p_{px} \cdot \frac{1}{g} \cdot \frac{F_{Detect}}{hc / \bar{\lambda}} QE \quad (11.)$$

Here, $\bar{\lambda}$ is the average wavelength of the considered wavelength band. Note that there is no subscript for F_{Detect} any more, we now just call it 'flux density'. This variable now refers to the energy per time over the complete wavelength band.

Whether an object can be detected in an image, depends on its *Signal-to-Noise Ratio* (SNR). That is the ratio of the signal, i.e. the asteroid, to the noise in the image. Assuming the number of incoming photons to follow a Poisson distribution, the 'photon noise' is simply \sqrt{DN} . Additional noise sources are:

- The readout noise of the output amplifier of the sensor;
- and the thermal noise generated during the exposure of the image, the so-called *dark current*. It is called like this as it is parasitic signal occurring even when the sensor is covered.

The readout noise is a function of the readout speed of the sensor. For typical astronomical sensors the readout is done slow enough to allow neglecting the readout noise.

$$SNR = \frac{DN_{signal}}{\sqrt{DN_{signal} + DN_{bias} + DN_{dark} + DN_{readout} + DN_{Sky}}} \quad (12.)$$

The dark current is a function of temperature and exposure time. Normally, professional cameras are cooled with liquid nitrogen to temperatures such that the dark current is negligible for the exposure times used for asteroid observations. For most cameras available on the amateur market, however, the dark current must be taken into account.

From ground-based telescopes the sky background plays a major role. The sky background is often given as a magnitude per square arcseconds. Even from good sites like the Tenerife observatory, the sky background typically corresponds to a brightness of 21 to 22 mag per square arcseconds.

We will here only briefly mention that normally all images obtained by a fixed camera-telescope combination need *calibration* to correct for the effects of uneven illumination over the field of view, for the varying noise characteristics of individual pixels, and the normally present offset of the readout signal in the sensor, the so-called bias. This is done by obtaining so-called *flat fields*, *dark frames*, and *bias frames*. The flat fielding would add an additional noise source in the formula given above. For a detailed description of image calibration see for example the excellent book by Berry and Burnell, *The Handbook of Astronomical Image Processing*.

9. Determining an asteroid's position from an image

Asteroids move with typically 0.1 – 10 arcseconds per minute in the sky. Close objects can be even faster. To measure the position of an asteroid, observers typically take three images of the same area of the sky shortly after each other. The exposure time of each individual image has to be short enough so

Task 2: The camera at ESA's telescope on Tenerife is cooled by liquid nitrogen to temperatures such that the dark current and its noise contribution can be neglected. The readout is slow enough so that also its noise contribution can be neglected. The camera is operated with a bias of $DN_{bias} \sim 4000$.

For a reliable detection, the SNR of an object should be larger than 5. Compute the sensitivity of ESA's telescope in magnitude, as described in Task 2, using the following assumptions for the CCD camera: $QE = 80\%$; $g = 0.9 \text{ e}^-/DN$. Assume that all the photons coming from the object are red at a wavelength of 600 nm. Assume that the telescope transmits $\tau = 80\%$ of the photons to the CCD; $p_{px} = 10\%$ of the photons fall on the center pixel. The telescope obstruction is 10% of the size of the main mirror.

that the movement of the asteroid does not smear out the asteroid's image over several pixel. To increase the signal-to-noise (SNR), one can stack several exposures which are shifted in the computer by the expected direction of movement of the asteroid. Then the stars will appear as short streaks, the asteroid will be a point source.

A technique called blinking is used to visually detect asteroids at the computer screen. Essentially one creates a short animation of the three images. If the asteroid is visible moving on an apparent straight line in all three images, a clear detection of the asteroid was done.

Automated systems essentially detect asteroids in the same way. However, also noise which is by

chance aligned on a straight line will be detected. Automated detection routines are less capable of detecting noise from a real asteroid image. Thus, most large surveys use four images or more to increase the robustness of the detection.

To compute an asteroid's orbit, its position relative to the stars needs to be known. For that, dedicated software exists, for example Astrometrica (see Figure 20). It works as follows:

An image (or a sequence of images) is read into the software. Normally, images are stored in the FITS format (FITS = Flexible Image Transport System). This is a format often used in astronomy, which allows storing meta-information in an ASCII header. Typical telescope/camera systems store the commanded pointing position of the telescope at the time of image acquisition in the FITS header as Right Ascension and Declination.

With this information, the software knows what the center coordinates of the image are. It will then search for brightness peaks in the image, which it assumes are stars. It compares the detected stars with the position and brightness of stars from a star catalogue. From comparing the x/y positions of the star centroids as measured in the image with the catalogue the software can determine the precise pointing, the image orientation, and the distortion of the optical system. The transformation coefficients from the x/y pixel position to celestial are called *plate constants*.

From those objects which are identified as asteroids – either manually or by an automated system from a set of images – the celestial coordinates can now be determined by applying the inverse transformation.

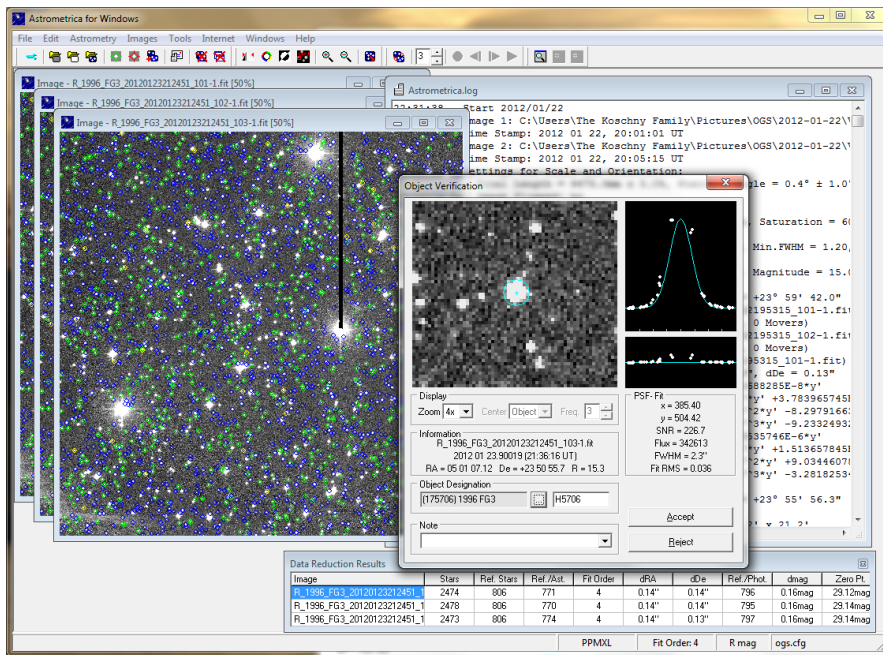


Figure 22: Screenshot of a typical astrometry software (<http://www.astrometrica.at>).

10. Follow-up – an important activity to keep track of where the objects are

Normally, possible asteroid impact risks can be ‘retired’ when more and better observations are obtained. For this reason frequent follow-up observations of these objects are necessary. Once discovered, objects can be followed even by smaller telescopes, say down to an aperture of 30-40 cm. Telescopes

in this size are available to many astronomical institutes, universities, and even to amateur astronomers who play a major role in this activity.

A number of tools are available to support follow-up activities. The MPC provides a web page¹¹ which lets an observer select the magnitude limit of his/her telescope and other observing constraints; it then produces a list of objects which can be observed from the observer's location. Another tool is the Spaceguard Central Node's priority list¹² – it checks the estimated uncertainty of an object's position and produces a table of observable objects which should urgently be observed in order to avoid that they get lost (i.e. their orbital uncertainty is so large that their predicted sky position at the next opposition would be larger than a typical telescope's field of view).

11. Orbit determination and first impact warning

11.1 Introduction

In this section, we give an example on how a preliminary orbit can be determined from several measured positions in the sky. The individual steps are the following:

The position of the observer has to be determined in inertial coordinates. We here use a Sun-centered ecliptic coordinate system. The celestial coordinates (right ascension, R.A., and declination, δ) of the asteroid in the image date represent the directions of the viewing vectors from the observer to the asteroid. Let these be available for at least two observations. Then the direction of the asteroid is known for these two observations, and the delta time in between the observations.

Solving this for an orbit uniquely is in principle only possible for a circular orbit. No unique solution can be found for two observations – the object could move perpendicular to the observer and be far away, or move towards to observer or away from him and be nearby, resulting in similar apparent velocities in the sky. Thus, good orbit solutions can only be found with more observations. To obtain an orbit with a reasonable accuracy, the object should have been observed for at least one, if not two complete orbits.

However, to determine the apparent positions of a newly discovered object at least in the next few days or weeks, even a rough orbit is of use. In the following, we will demonstrate how such an orbit can be determined by using the method of Herget.

11.2 Converting celestial coordinates to inertial vectors

For performing transformations between different coordinate frames, it is useful to remind one of the standard rotation matrices for vectors:

$$\begin{aligned}
 R_x(\alpha) &= \begin{bmatrix} 1 & 0 & 0 \\ 0 & \cos \alpha & -\sin \alpha \\ 0 & \sin \alpha & \cos \alpha \end{bmatrix} \\
 R_y(\beta) &= \begin{bmatrix} \cos \beta & 0 & \sin \beta \\ 0 & 1 & 0 \\ -\sin \beta & 0 & \cos \beta \end{bmatrix} \\
 R_z(\gamma) &= \begin{bmatrix} \cos \gamma & -\sin \gamma & 0 \\ \sin \gamma & \cos \gamma & 0 \\ 0 & 0 & 1 \end{bmatrix}
 \end{aligned} \tag{13.}$$

¹¹ <http://scully.cfa.harvard.edu/cgi-bin/neaobs.cgi>

¹² <http://spaceguard.iasf-roma.inaf.it/SSystem/SSystem.html>

where α is a rotation about the x-axis, β about the y-axis, and γ about the z-axis. Assume a vector $\vec{r}_1 = [x, y, z]$. Assume this vector is given in a coordinate system 1. Coordinate system 2 is shifted by vector \vec{s} and rotated by angles a, b, and g. Then, \vec{r}_2 can be determined by

$$\vec{r}_2 = \vec{r}_1 R_x R_y R_z \quad (14.)$$

Note that the order in which the rotations are applied are important.

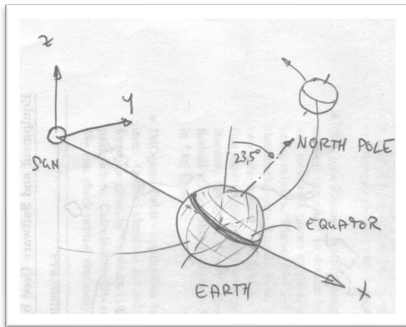


Figure 23: Converting celestial to inertial coordinates.

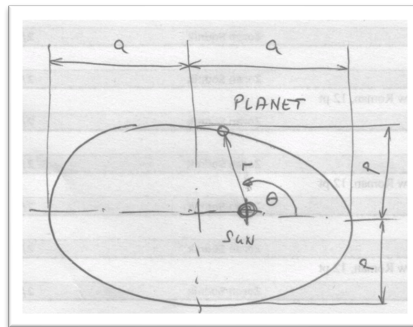


Figure 24: A Kepler ellipse.

Inspect Figure 23. Assume that the Earth is at its vernal equinox position. That is when the x-axis of the inertial coordinate system goes through the center of the Earth and its equator. Converting celestial coordinates as seen from the Earth at this epoch (time) means to rotate the coordinate frame by 23.5° (the obliquity of the Earth) about the x-axis and shift the coordinate frame by the distance between Earth and Sun in the x-direction.

At any other point in time, the rotation stays the same, but the transformation will be in x and y direction, depending on the position of the Earth in its orbit (for simplicity, we assume that the observer is located at the center of the Earth. In real life, one would need to compute the x/y/z coordinates of the observer relative to the Earth's center from the observer's geocentric location and the time of observation).

11.3 The position of the Earth as a function of time

To compute the position of the Earth as a function of time after vernal equinox (21 March), we use the following formalism. Kepler showed, based on Newton's laws of motion that planets orbit around the Sun in an ellipse:

$$r = \frac{p}{1 + \epsilon \cos \theta} \quad (15.)$$

Where r is the distance between the Sun and the Earth, p the semi-latus rectum (Figure 24), and ϵ the eccentricity:

$$\epsilon = \frac{r_{\max} - r_{\min}}{r_{\max} + r_{\min}} \quad (16.)$$

To determine the position (r, θ) of the Earth as a function of time, we use the so-called mean anomaly M . It is defined as the angle which a fictitious object would move in time t which has the same orbital period P as our planet of interest, see Figure 25. The mean anomaly as a function of time can then simply be written as

$$M = \frac{2\pi \cdot t}{P} \quad (17.)$$

P is the period of the orbit, t the time after pericenter. From Kepler's second law, it can be derived that the eccentric anomaly, as defined in Figure 25, can be written as

$$M = E - \varepsilon \sin E \quad (18.)$$

This is a transcendental equation which can be easily solved by iterative methods. From E , the so-called true anomaly θ can be derived as

$$\tan \frac{\theta}{2} = \sqrt{\frac{1+\varepsilon}{1-\varepsilon}} \cdot \tan \frac{E}{2} \quad (19.)$$

With these formulae, the position of the Earth ($r(t)$, $\theta(t)$) can be computed as a function of time.

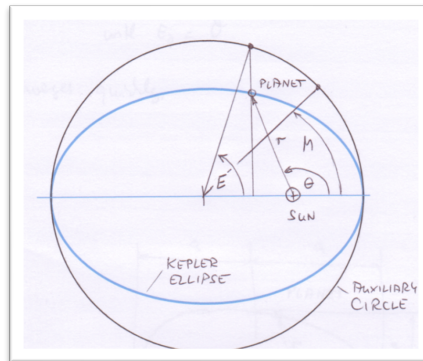


Figure 25: The true and eccentric anomaly θ and E .

The vector to the asteroid is then simply the position of the Earth at time t plus the direction to the asteroid as computed from the right ascension and declination of the observations.

11.4 Converting to a state vector

The *state vector* we call the six-element vector of a solar system object giving its position in x/y/z coordinates (typically in a Sun-centered ecliptic coordinate system) and its velocities v_x , v_y , v_z . In many real computational cases it is important to convert the \vec{r} , \vec{v} obtained in the previous section to the state vector as for example distances between objects can then easily be computed.

In this version of the script, we refer the reader to the textbook by Walter (2008) where this conversion is derived in Section 14.4.2.

11.5 Applying the method of Herget to estimate radius and velocity vectors

The method of Herget works as follows. As input, the directional vectors of two asteroid positions are used, including the delta time between them. The starting value for the distance of the Sun is guessed. We now have two points in inertial space which need to be connected by a Kepler orbit. There is only one orbit solution which can take the object from P_1 to P_2 in the time t . Thus, we start by 'guessing' v_1 :

$$\vec{v} = \Delta r / \Delta t \quad (20.)$$

Without gravity this would be correct. To perform a better estimate, gravity should be included to the first order. To do this, we compute the acceleration of the object at the midpoint $\vec{r}_1 + \vec{r}_2 / 2$ between the two positions:

$$\vec{v}_1 = \frac{\Delta \vec{r}}{\Delta t} - \vec{a} \frac{\Delta t}{2} \quad (21.)$$

Now the orbit is numerically integrated from t_1 to t_2 . The end result will *not* be \vec{r}_2 . So, if the solution is off by an amount Δr , a new guess for the velocity should be calculated:

$$\vec{v}_{1,new} = \vec{v}_1 \frac{\Delta \vec{r}}{\Delta t} \quad (22.)$$

Steps (19) to (21) are repeated until the difference in r is sufficiently small.

11.6 Convert these to orbital elements

The orbital elements are defined in Figure 26. In that diagram, the inertial Sun-centered ecliptic coordinate system is denoted with the unit vectors $\vec{I}, \vec{J}, \vec{K}$. The angular momentum vector \vec{h} is perpendicular to the orbit. \vec{n} denotes the line of nodes with the vector pointing to the ascending node.

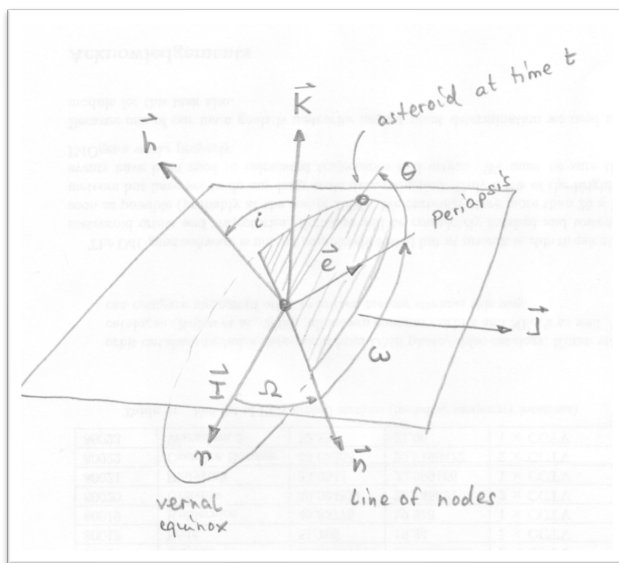


Figure 26: Definition of orbital elements.

We can determine the orbital elements from the position and velocity vector the following way.

Compute the angular momentum vector:

$$\vec{h} = \vec{r} \times \vec{v} \quad (23.)$$

The line of nodes is in the plane of the orbit and in the plane of the ecliptic. In other words, it is perpendicular to both the angular momentum vector and vector \vec{K} :

$$\vec{n} = \vec{h} \times \vec{K} \quad (24.)$$

The so-called eccentricity vector \vec{e} is defined as

$$\vec{e} = \frac{1}{\mu} \left[\left(v^2 - \frac{\mu}{r} \right) \vec{r} - (\vec{r} \cdot \vec{v}) \vec{v} \right] \quad (25.)$$

The length of the vector corresponds to the eccentricity of the orbit ellipse. For a derivation of this formula, see Bate *et al.* p. 25.

$\mu = GM$ with G the gravitational constant ($G = 6.67 \cdot 10^{-11} \text{ m}^3\text{kg}^{-1}\text{s}^{-2}$) and M the central mass – in our case the mass of the Sun ($M = 1.98892 \cdot 10^{30} \text{ kg}$).

With these three vectors, and noting that the dot product of two vectors allows determining the angle between the two vectors

$$\begin{aligned}\vec{A} \cdot \vec{B} &= AB \cos \alpha \\ \cos \alpha &= \frac{\vec{A} \cdot \vec{B}}{AB}\end{aligned}\quad (26.)$$

we can now determine the orbital elements:

$$p = h^2 / \mu \quad (27.)$$

The inclination i is the angle between \vec{K} and \vec{h} :

$$\cos i = \frac{h_K}{h} \quad (28.)$$

The inclination is always less than 180° , thus no checking of the quadrant needs to be done.

The right ascension of the ascending node, Ω , is the angle between \vec{I} and \vec{n} , thus

$$\cos \Omega = \frac{n_I}{n} \quad (29.)$$

Here a check must be made whether $n_I > 0$; then Ω is less than 180° .

The argument of periapsis is the angle between the line of nodes and the direction of the eccentricity vector:

$$\cos \omega = \frac{\vec{n} \cdot \vec{e}}{n e} \quad (30.)$$

If $e_K > 0$, then ω is less than 180° .

The true anomaly is the angle between the direction of periapsis and the radius vector:

$$\cos \theta = \frac{\vec{e} \cdot \vec{r}}{e r} \quad (31.)$$

If $\vec{r} \cdot \vec{v} > 0$ then θ is less than 180° .

With these equations, the orbital elements of an object can be determined from its initial observations. Note that the method of Herget only gives a first estimate of the orbit – to do a more precise orbit determination, more complex methods should really be used. With the explanations given here the principle should have become clear:

1. Measure at least two positions of the asteroid in celestial coordinates;
2. Compute the position of the Earth in a Sun-centered ecliptic coordinate system;
3. Using an assumed distance to the asteroid, compute the position vectors of the asteroid in the Sun-centered ecliptic coordinate system from 1 and 2;
4. Apply the method of Herget to estimate better position vectors and a velocity vector;
5. Convert the position and velocity vector to orbital elements.

Using the orbital elements and equations (15) to (19) for the asteroid, its position as a function of time can be computed. From this, also the Minimum Orbital Intersection Distance (MOID) can be estimated.

Tools for a more thorough orbit analysis are freely available on the internet. See for example the software 'find_orb' written by William Gray¹³. It will read position measurements of asteroids and compute orbits using different methods.

11.7 Non-gravitational forces

There are a number of non-gravitational forces which may affect the orbit of objects in the solar system. For asteroids, the major effect is the so-called Yarkowsky effect. It is related to the heating of the asteroid by the Sun and the uneven emission of thermal radiation because of the rotation of the object.

The radiation of the Sun will heat up the asteroid, mainly at the sub-solar point. The asteroid re-radiates this energy in the thermal infrared. For a non-rotating asteroid, this re-radiation would be pointed towards the Sun. For a rotating object, the re-radiation will be in a different direction. For objects rotating in a prograde direction (*i.e.* with the same orientation as their orbital direction around the Sun) this radiation will be roughly opposite to the direction of motion of the object. It will have the effect of very slightly increasing the velocity of the asteroid, resulting in the object to increase its semi-major axis. A retrograde rotation will result in a decrease of the semi-major axis.

These effects are extremely small – but have been measured for a handful of asteroids. They are important in the prediction of asteroid impacts. In particular when taking keyholes into account (see the following section), a very small change of the objects position at one Earth flyby may result in the object impacting at the next Earth flyby.

11.8 Keyholes

A *keyhole* is a position in space during the flyby of an asteroid at the Earth, where it would be deflected such that it would impact the Earth at its next flyby. A simple way of visualizing a flyby is by defining the so-called *modified target plane*. This is the plane going through the center of mass of the target object and perpendicular to the velocity vector during the closest approach. However, asteroid scientists and mission analysts normally prefer to use the *B-plane* or simply *target plane*. The B-plane is the plane through the center of mass of the target body (in our case the Earth), perpendicular to the velocity vector \vec{v} outside the sphere of influence of the Earth. This definition has certain advantages in particular for taking into account the gravitational influence of the target body. It does mean that the impact cross-section B of the target body is larger than its real radius:

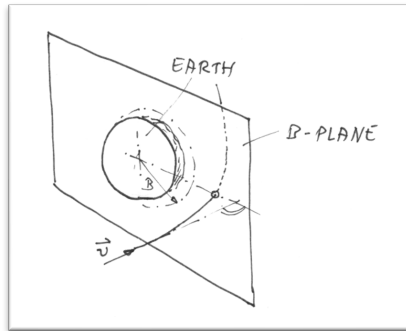


Figure 27: Definition of the B-plane.

$$B = R\sqrt{1 + 2\mu / Ru^2} \tag{32.}$$

where R is the radius of the Earth. Figure 27 shows the definition of the B-plane graphically. A coordinate system (ξ, η, ζ) in the B-plane is defined such that the negative ζ -axis is aligned with the projection on the target plane of the heliocentric velocity of the planet \vec{v} and the positive η points along the direction of the asteroid velocity.

The keyholes for Apophis during its next flyby at the Earth in 2029 are shown in Figure 28. If the asteroid were to fly through one of the points marked with a year, it would be deflected such that it would impact the Earth in the given year.

¹³ http://www.projectpluto.com/find_orb.htm

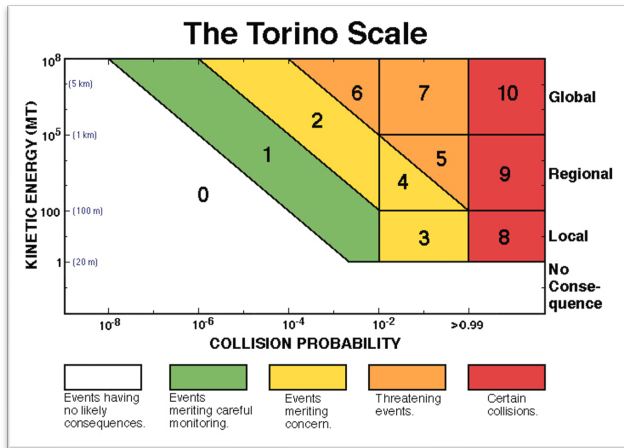


Figure 29: The Torino impact hazard scale. Credit: Binzel 1999.

11.9.2 Palermo scale

The Palermo Scale (PS) was developed to quantify the risk of an asteroid impact for the scientific user. A rating of 0 means the hazard is as likely as the background hazard (defined as the average risk posed by objects of the same size or larger over the years until the date of the potential impact). A rating of +2 would indicate the hazard is 100 times more likely than a random background event. Scale values less than -2 reflect events for which there are no likely consequences, while Palermo Scale values between -2 and 0 indicate situations that merit careful monitoring (Chesley *et al.* 2002).

The Palermo scale value can be computed with the following equation:

$$PS = \log_{10} \frac{p_i}{f_B T} \quad (33.)$$

where PS : the Palermo scale value; p_i the probability of impact; $f_B = 0.03 E^{-0.8}$ the annual background impact frequency with E the impact energy in megatons TNT (this is an energy unit just like Joule – see the next section for an explanation), and T the time to the impact in years.

Task 3: The asteroid 2008 TC₃ entered the Earth's atmosphere over Sudan in Oct 2008 and exploded in about 20 km altitude. A number of meteorites were found which came from the object. Its estimated size corresponds to a sphere of radius 4 m. Its velocity was measured in space to be 15 km/s relative to the Earth. The density of the meteorites recovered after the explosion was around 2.5 g/cm³.

Assume that the complete kinetic energy was converted into explosive energy. How many Hiroshima bombs would be needed to generate the same explosive force?

Task 4: What would have been the Palermo scale (PS) value of this object one year before the impact? What is the PS value of the currently most dangerous object? Check on the NEODYs 'risk page'. Would the Sudan event have a higher or a lower value?

To understand the relation given for the background probability, jump to Figure 36. In a double-logarithmic diagram the frequency of impact plots as a straight line. The slope of this line is the value of -0.8. Compute the probability for $E = 1 \text{ Mt}$ – it is 0.03 per year, or one impact every 33.3 years. Draw a line from an impact energy of 1 Mt upwards until it intersects the dashed frequency distribution. Read of the impact interval on the right side of the plot – it will be 33.3 years.

11.9.3 Megaton/kiloton TNT

The energy which is released upon an impact is often given in *megatons TNT* or *kilotons TNT*. This is normally used by the military for explosions and can be converted to Joule by the following relation:

$$1 \text{ kt (kiloton TNT)} = 4.184 \cdot 10^{12} \text{ J} \quad (34.)$$

It is the energy that is released when 1000 tons (10^6 kg) Trinitrotoluol explode.

To put this number in context: The largest bomb ever used was the so-called Zar-bomb. It was a Russian hydrogen bomb with an explosive yield of about 50 Mt. The Hiroshima bomb had a yield of about 15 kt.

11.10 Orbit propagation

For a simple Kepler orbit, the position of the asteroid would be predictable far into the future by applying the equations defined in Section 11.3 to the orbital elements determined for the asteroid. In reality, however, asteroids are affected by the gravity of all planets. For NEOs, the Earth itself obviously affects the orbit: After a close flyby to the Earth, the orbital elements can be dramatically changed (thus the concept of ‘keyholes’ as discussed in Section 11.8). Even non-gravitational effects may play a role, such as the Yarkovsky effect discussed in a later section.

Therefore, the current impact prediction tools – NEODyS in Europe and SENTRY in the US – use numerical propagators to determine the position of the asteroid in question. Both NEODyS and Sentry currently propagate orbits 100 years into the future. At the time of writing this document, both tools only take gravitational effects into account.

11.11 The Yarkovsky effect

One of the major non-gravitational effects influencing the orbit of asteroids in the size range of meters to tens of kilometers is the *Yarkovsky effect*. The unsymmetrical emission of thermal photons will result in a force acting on the orbit. The effect was first published by Öpik (1951). He stated that he found the effect described in a non-

Task 5: (a): What is the typical angular velocity in arcsec/min of a main-belt asteroid as seen from the Earth when the object is in opposition?

Assume a distance to the Sun of 2.5 au, circular orbit.

(b): ESA’s 1-m telescope is an f/4.4 system. The CCD camera has a pixel scale of 13.5 μm . If you want to limit the image smear to less than 1.5 pixel, how long can your maximum exposure time be?

(c): How long will it take for a main-belt object of 100 m and average thermal conductivity and $a = 2.2 \text{ au}$ to drift to the next resonance?

(d): What is needed to predict the Yarkowsky effect?

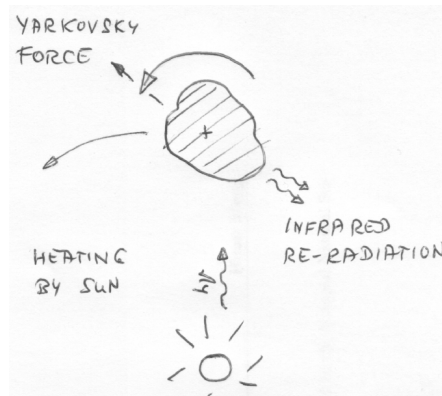


Figure 30: Visualization of the Yarkovsky effect.

published manuscript by the Polish/Russian civil engineer Yarkovsky.

Recent descriptions of this effect go back to papers by Vokrouhlický (e.g. 1998). There are two major contributions to the effect – the diurnal and the seasonal effect.

The diurnal effect can be explained as follows: Assume an asteroid is rotating and has a certain heat capacity. The solar radiation will heat the asteroid. This heat is re-radiated from the asteroid by infrared photons. If the asteroid were always facing the same side to the Sun, this part would be the hottest. The re-radiation would be in the direction of the Sun, slowly pushing the asteroid outwards. Because of the rotation and the finite heat capacity of the asteroid, this re-radiation will be in a different direction, namely shifted to the dusk side of the object, i.e. in the direction of the rotation. If the rotation is prograde, the shift will be opposite the direction of motion of the asteroid. It will act as a force increasing the speed of the object, thus increasing the semi-major axis of the object. A retrograde rotation will have the opposite effect.

This force is very small, in the order of Newtons. However, since it acts continuously over Millions of years, it may have a non-negligible effect. It is one of the effects deemed responsible for moving main-belt asteroids into resonance areas, from where they are then deflected such that they become NEOs.

As the effect is depending on a large number of parameters (rotation speed, spin axis orientation, thermal properties of the asteroid) it is very difficult to predict. It is currently not part of the standard impact prediction tools like NEODyS.

We will not discuss the mathematical derivation of the problem here, the interested reader is referred to the paper by Vokrouhlický (1998).

12. Physical properties characterization

An attempt to give a complete list of physical properties of an asteroid is done in Table 2. The different measurement possibilities are given in Table 3. Table 2 links the two and shows in the center column which measurements need to be performed to allow the determination of these properties.

Obviously, the best characterization is done *in-situ*, i.e. by a spacecraft orbiting and possibly even landing on the asteroid. So far, 12 asteroids and/or comets have been visited by spacecraft (Figure 31). Only one object, asteroid (433) Eros, has been orbited by a spacecraft (Figure 7).

The ultimate characterization can be done by returning a sample from an asteroid to the Earth. The European Space Agency studied such missions in 2008/2009 and 2011-2013, called Marco Polo and MarcoPolo-R, respectively. The US is currently implementing such a mission, called OSIRIS-REx. It will return a sample from asteroid 1999 RQ₃₆.

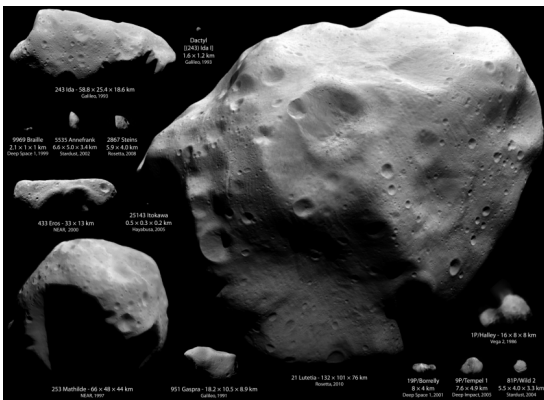


Figure 31: All asteroids visited by a spacecraft - missing only Vesta, where the US spacecraft Dawn only arrived last year. Credit: Planetary Society.

Table 2: Physical properties of asteroids.

Physical property	Measurement (Table 3)	Comment
Orbit	(1)	
Rotation period	(6), (10)	For radar only possible under certain geometries
Orientation of spin axis	(6), (10)	For radar only possible under certain geometries
Size	(3), (4), (5)	Albedo can be estimated from infrared observations, more precisely from thermal infrared observations. Then the size can be computed from absolute magnitude measurements. The degree of polarization as a function of phase of the asteroid can also be used to determine the albedo.
Shape model	(6), (10)	Needs extended light curve observations
Mass	(1), (3), (5), (6), (10), (11), (12)	For some (few) asteroids, the mass of them can be estimated by their perturbation of other asteroid's orbit. The mass can be estimated quite well for binary systems from the rotation period of the secondary.
Gravity field	(1), (3), (5), (6), (10), (11), (12)	Can be estimated from size and a guess for the density. For more precise measurements an orbiting spacecraft is needed.
Binary properties	(6), (10)	These are mass ratio, distances, periods.
Dust environment	(8)	

Table 3: Measurement method.

Number	Measurement method	Comment
(1)	Astrometry	Imaging with telescope, no filter needed
(2)	Direct imaging	To resolve the disk – Hubble telescope or a very small number of ground-based observations using adaptive optics
(3)	Spectroscopy	Visible and infrared
(4)	Thermal infrared observations	Only possible space-based, e.g. with the Spitzer telescope
(5)	Polarimetry	
(6)	Light-curve measurements	Repeated imaging with telescope – for absolute magnitude determination two spectral ranges needed
(7)	Phase curve measurements	Imaging with telescope under different phase angles of the asteroid
(8)	Long exposure imaging	
(9)	Radar ranging	Goldstone and Arecibo radio telescopes; in Europe only demonstrated with Evpatoria and Sardinia radio telescopes (E. as transmitter). Should be possible with TIRA radar in Germany. Needs close flyby of asteroid (< ~Mio km)
(10)	Radar Doppler imaging	Goldstone and Arecibo radio telescopes
(11)	Spacecraft flyby	
(12)	Spacecraft orbiting	
(13)	Spacecraft landing	

For more detailed information, a good starting point is the web page of a recent workshop on the physical characterization of spacecraft mission target asteroids, held in January 2012 in Meudon, France¹⁴. It contains links to a number of presentations dealing with the ground-based physical characterization, mainly of asteroid 1996 SF₃, the target asteroid for ESA's MarcoPolo-R mission study.

To give at least one example for how to deal with physical property measurements, we show how the data from three night's observations of 1996 FG₃ by one of the authors (DVK) can be used to determine the rotation period of the asteroid.

12.1 Obtaining the observations

This section will be added in a future revision of the document. For now, refer to the class presentation "Lecture 3 – Physical properties".¹⁵

12.2 Measuring light curves

Visualize an ellipsoidal asteroid in space, rotating about an axis perpendicular to your viewing direction. Assume that the phase angle is close to zero, *i.e.* that your observing location is close to the Sun-asteroid line (Figure 32). If the object points the broad side towards you, a much larger area of the object will reflect light back to you than if it points the narrow side to you. Given a constant rotation rate P , the light intensity will change with $2P$ (Figure 33).

For a camera located in space, outside the Earth's atmosphere and in stable conditions, measuring an asteroid light curve can be as simple as repeatedly taking images of the object, using the same exposure time. By measuring the Digital Number of the asteroid in a certain aperture around the photometric center of the object, the light curve can be recorded.

In order to get an absolute brightness value, the Digital Number has to be calibrated using known field stars. Care has to be taken due to the color of the reference stars. If the reference star does not have the same color (*i.e.* the same spectral density distribution) as the Sun, the derived magnitude values will be off.

An additional complication arises for ground-based telescopes. The atmosphere around our planet not only attenuates the received light, it also does this as a function of object elevation, and differently for different wavelength bands. To obtain precise magnitude measurements of asteroids (or any object in

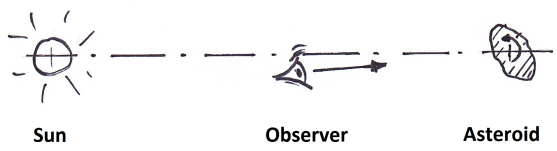


Figure 32: Observing conditions for the situation described in the text.

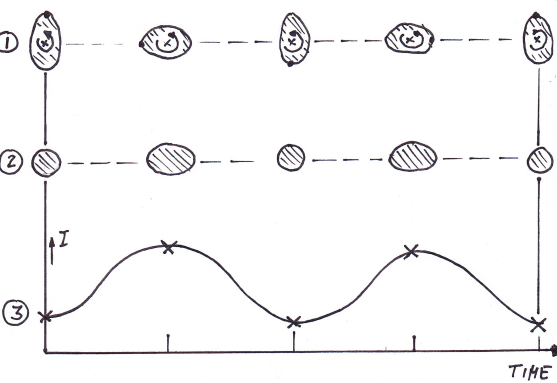


Figure 33: The light curve of an asteroid: (1) shows the rotational state in a 'top view', (2) is the view as seen from the observer. (3) shows the resulting reflected sunlight intensity, the so-called light curve.

¹⁴ <http://smass.mit.edu/MarcoPolo/home.html> (last accessed: 03 Mar 2012).
¹⁵ Available at <http://neo.koschny.eu>

the sky, for that matter), all this needs to be properly calibrated out. An excellent and reasonably short summary on how to do this can be found in Buchheim (2007), Section 4.

12.3 Deriving the rotation period

This section will be added in a future revision of the document. For now, refer to the class presentation “Lecture 3 – Physical properties”.

12.4 Spectroscopic observations

A common technique to learn something about the composition of an object is to use spectroscopic observations. Using a prisma or a grating, the light coming from the object is split up into different wavelengths. The reflected light intensity can then be plotted as a function of wavelength.

Figure 34 shows the currently adopted standard 'taxonomy', i.e. grouping of spectra. The x-axis is the wavelength, the y-axis the intensity. I.e. a so-called S-class asteroid has a spectrum which increases small to larger wavelengths (i.e. from blue to red). It also has a few absorption bands.

Bus and DeMeo (2009) have produced this classification after performing measurements on a large sample of asteroids. These measurements can now be compared with ground-based reflectance spectra of meteorites. This allows linking meteorites with asteroid classes.

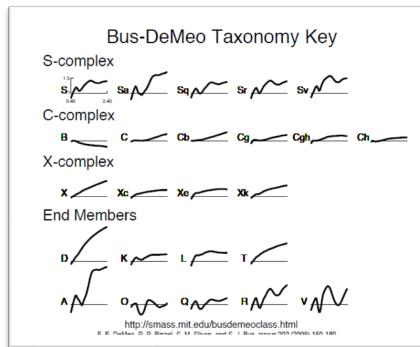


Figure 34: Typical spectra of asteroids - the x-axis is the wavelength, the y-axis the intensity of the reflected light.

12.5 Temperature of an asteroid

The temperature of an asteroid can be computed if its albedo is known via the 'Standard Thermal Model (STM)' (Lebofsky et al. 1986):

$$T(0) = \left[(1 - A) F_{ast} / (\eta \epsilon \sigma) \right]^{1/4} \quad (35.)$$

The temperature $T(\theta)$ at the sub-solar point can be computed using the solar flux density at the asteroid in W/m^2 , F_{ast} , knowing the following parameters: A = albedo, η = the so-called beaming factor - it takes into account the observed enhancement of the temperature at small phase angles, ε = emissivity of the asteroid's surface, σ = Stefan-Boltzmann constant ($5.67 \cdot 10^{-8} \text{ Wm}^{-2}\text{K}^{-4}$).

The parameter η was initially introduced to allow fitting measurements to observations. η is a measure of how homogeneous the temperature distribution on the asteroid is, *i.e.* how much of the heat will be retained close to the surface area just 'below' the Sun. The subsurface temperature will be higher for rougher surfaces, lower thermal conductivity, and lower rotational period with typical values of $\eta = 0.5 \dots 3.0$ (Harris and Drube 2014).

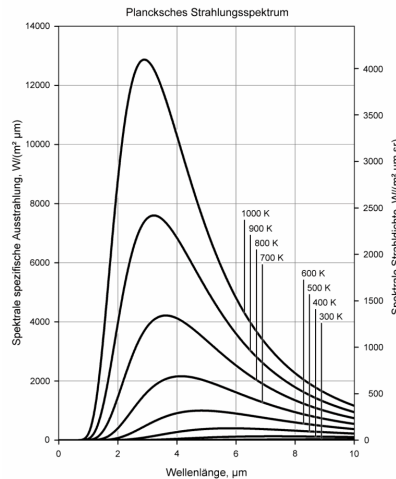


Figure 35: Black body emission at different temperatures.

12.6 Thermal observations

'Thermal observations' stands for the observation of asteroids in the near- and thermal infrared. These observations are very important for the determination of the impact threat. They allow a fairly accurate determination of the albedo of the object, and thus allow the determination of the asteroid size. This is how it works:

Task 6: Using the Stefan-Boltzmann law and the 'Standard Thermal Model', estimate the temperature of an asteroid at 1 AU and 2 AU distance to the Sun. Assume the emissivity ε of regolith: 1.0; use albedo $A = 0.04$ (primitive asteroid) and 0.4 (Steins).

Assume that you observe an asteroid in the visible. A direct measurable at the telescope is the apparent magnitude of the object. If you have enough position measurements to do compute the orbit, you know the distance of the object at the time of observation. If you knew the percentage of light that the object reflects (the albedo), you could compute precisely the surface area and thus (assuming a spherical body) the diameter of the object. Unfortunately the albedo is not known precisely and often a value of 0.15 is assumed.

Enter the thermal infrared measurements. We know that the temperature of an asteroid is somewhere between 100 and 400 K. The precise value depends on the size of the body and the albedo. The black-body radiation has a peak at wavelengths between 8 to 14 μm - which is precisely what we can measure in the thermal infrared (see Figure 35). Thus, from thermal infrared measurements we can determine the temperature of an asteroid.

Assume you have determined the absolute magnitude of an object. Since you don't know what the albedo is, the object could be either large and dark, or small and bright. The temperature allows you to find out which - a large object will collect more energy from the Sun. It is dark, thus it will absorb a lot of energy. As a consequence it will be quite warm. A small, bright object, on the other hand, collects less sunlight and will reflect more. It will be cooler.

When measuring the absolute magnitude and the temperature of an asteroid at a given distance to the Sun, you can then work out the precise value of the albedo and the size.

12.7 Radar observations

Radar systems can be used to observe asteroids. There are two main types of radars:

- All-sky radars, normally based on large arrays of antennas. These emit power over the complete sky, thus their actual power density is not very high. They are typically used for observing satellites or space debris in low to medium Earth orbits.
- Radars using dish antennas. These allow emitting power in a very small cone into the sky. Almost all observations of asteroids with radar systems have been done with two antennae, namely the Goldstone radar in the US and the Arecibo radar in Puerto Rico.

Using a technique called Doppler-delay imaging, the shape of the asteroid can be resolved for objects sufficiently close. Typical maximum distances for asteroids are several million kilometers. To just obtain a precise distance to the asteroid, distances can be larger.

Due to the small size of the cone in which a radar emits power, the position of the observed asteroid must be known reasonably well, say to better than a few arcminutes in the sky. Radars are thus not used for finding new objects; rather they are used to characterize objects which come close enough to our planet to reflect sufficient signal.

The key item to know when it comes to radar observations is the so-called *radar equation*. It links the received power from an object to the emitted power and the object properties. A derivation of the radar equation can be found atv. The equation looks like this:

$$P_{received} = \frac{P_{emit} G A_{radar}}{(4\pi)^2 R^4} A_{Antenna} K_a \quad (36.)$$

Here $P_{received}$ and P_{emit} are the received and emitted power, respectively (in W).

G is the gain of the antenna. This can be interpreted as the ‘focussing factor’. An antenna emitting over the complete sky (2π steradian) has a gain of 1. A_{radar} is simply the collecting area of the receiving radar. R is the distance to the object, K_a is the efficiency of the antenna.

For deriving this equation see <http://www.radartutorial.eu/01.basics/rb13.en.html>.

13. Impact probabilities and consequences

Probably the most famous impact event happened 65 Million years ago, at the so-called KT boundary (KT = Cretaceous/Tertiary). It led to the extinction not only of the dinosaurs, but to about 70 % of life in existence in those days. It is estimated that the object that hit the Earth to produce these effects had a size of about 10 km. In 1908, an object of about 30–40 m in size exploded above the Tunguska area in Siberia. It flattened about 2000 km² of trees. Had it occurred over inhabited area its consequences would have been fatal. An object of this size is expected to occur about once every few hundred years. Up until a few years ago, scientists expected any object smaller than that to never reach the ground. They were proven wrong in 2007, when a normal rocky object (an ‘ordinary chondrite’) of only ~1 m in size penetrated the atmosphere in Carancas, Peru, reached the surface, and produced a crater of about 14 m in diameter. Scientists still try to understand why such a small object could reach the ground and did not fragment in the air; most likely it was the rather shall entry angle of the meteoroid (Tancredi *et al.* 2008).

Task 7: Assume that for ‘imaging’, the Arecibo radio antenna needs to be able to detect at least $P_{received} = 1e-16$ W. What is the largest distance in which it can image an asteroid with 100 m size?

As an emitter, the Goldstone antenna is used. It has a 400 kW emitter (effectively $P_{emit} = 400$ GW in pulsed mode). The gain is 80 dB. The effectivity of the Arecibo receiver is $K_a = 0.7$, its diameter 300 m.

Figure 36 shows a plot of the probabilities of impacts according to Harris 2007¹⁶. According to this diagram, an object the size of the Tunguska impactor would hit the Earth about once every few hundred years. A 1-m object would hit once every year.

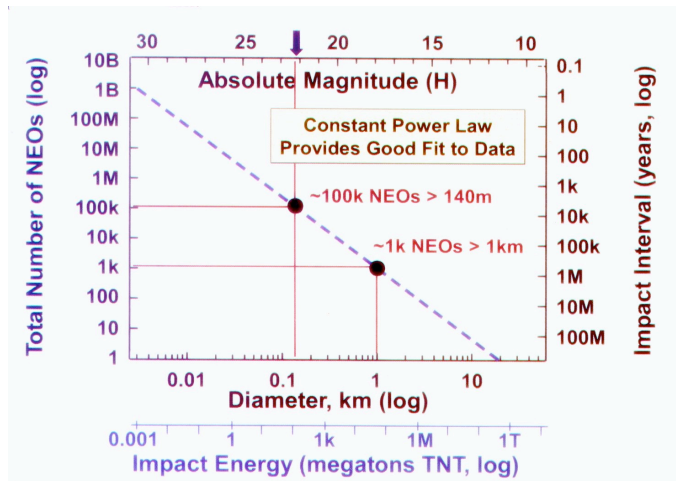


Figure 36: Impact probabilities according to Harris 2007. Harris estimates about 100000 objects with a size of 140 m, with one chance in ~2000 years that one of them hits the Earth. A 10 m object would hit the Earth roughly once per 10 years. There are indications that in the size range between meters and decimeters, the actual numbers are higher than those predicted by the straight line fit (Brown *et al.* 2013).

As a general rule, asteroids produce damage as a function of their kinetic energy, thus size, velocity, and density. While several studies on impact effects have been carried out, the uncertainties on the effects of an asteroid hitting the Earth are larger than the estimates of this to actually happen. See *e.g.* Collins *et al.* (2005) for a discussion.

When an asteroid reaches the Earth, the following regimes can be distinguished:

- (a) Atmospheric entry
- (b) Effects of an atmospheric explosion
- (c) Impact on the ground or water
- (d) Long-term effects

What will happen in these different regimes depends on the size of the object. For small objects (as mentioned before – previously thought for objects below ~40 m) the object will ablate in the atmosphere and most likely explode some height above the ground.

14. Decision process for impact threat mitigation

In 1999, the issue of the NEO threat came to the attention of the United Nations. In 2001, the ‘Action Team 14’ was installed, which was given two tasks: In a first phase until 2008, to produce a summary of existing activities on dealing with the NEO threat; in a second phase from 2008 to 2013, to actually develop draft recommendations for the Scientific and Technical Subcommittee of the UN COPUOS¹⁷ (Committee on the Peaceful Uses of Outer Space) on how to react in case of an imminent asteroid impact threat. If endorsed by the Subcommittee, the recommendations would be passed on for

¹⁶ <http://www.aero.org/conferences/planetarydefense/2007papers/S1-3--Harris-Brief.pdf>

¹⁷ <http://www.oosa.unvienna.org/oosa/en/COPUOS/copuos.html>

consideration by COPUOS. If COPUOS endorses the recommendations, they move to the UN General Assembly for consideration.

The second phase (the *implementation* phase) started from a report written by the Association of Space Explorers (ASE¹⁸). The ASE is a non-profit organization whose members are all astro/cosmo/taikonauts. In 2008, the ASE wrote a report called 'Asteroid threats: A call for global response'¹⁹. This report gave some first ideas on how to set up a global asteroid warning network and how to derive a decision process for action in case of an impact threat. These workshops and discussions have been supported by two non-profit organizations: The Association of Space Explorers, and the Secure World Foundation²⁰. Local organization of the workshops were done by different institutions. While initially the Regional Center for Education in Space Science and Technology in Latin America and the Caribbean (CRECTEALC), the European Space Agency (ESA), and the US space agency NASA contributed significantly, in the end the discussions were truly international, involving all major space-faring countries of the world.

This report had been the baseline for a discussion in many meetings during the COPUOS sessions and in additional workshops. On 15 Feb 2013, the final recommendation was presented to the Scientific and Technical Subcommittee of COPUOS, accepted by COPUOS itself in June 2013 and adopted by the

UN General Assembly in Dec 2013. The concept is depicted in Figure 37.

Two groups have been installed: An 'International Asteroid Warning Network' (IAWN) and a Space Missions Planning Advisory Group (SMPAG).

The International Asteroid Warning Network

The IAWN is a network of experts that focusses on discovery, tracking, and the observation of NEOs. The goal will be to find objects as early as possible. Observations are processed and orbit predictions and any potential impact warnings are generated. The IAWN will also prepare public communications. In case of a credible impact threat, IAWN will ensure that more information on these objects is gathered expeditiously. IAWN will then also inform COPUOS and the Office of Outer Space Affairs (UN OOSA). The IAWN consists of observers, astrodynamics experts, experts working on the

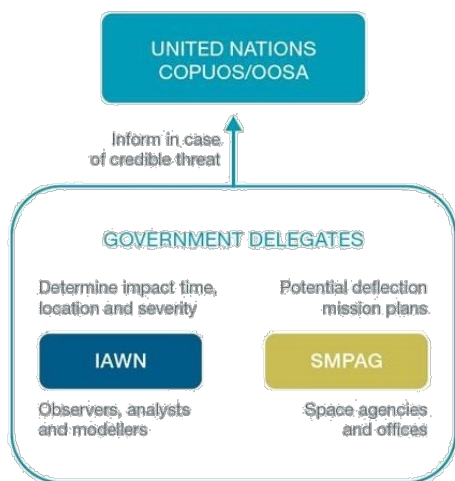


Figure 37: The UN setup for deciding on what to do in case of an imminent asteroid impact threat.

characterization of asteroids and modeling. No formal 'group' is needed; it is a network of existing experts and assets. A steering group for the IAWN has been formed during a meeting in Baltimore, USA, in Jan 2014. This steering group acts a focus point for the IAWN. COPUOS will receive yearly summary reports from the IAWN.

¹⁸ <http://www.space-explorers.org>

¹⁹ <http://www.space-explorers.org/ATACGR.pdf>

²⁰ <http://swfound.org/>

The IAWN will also work on establishing interfaces to the international emergency response agencies. The Minor Planet Center in Cambridge, USA, maintains a web site for the IAWN²¹.

The Space Missions Planning Advisory Group

The SMPAG combines the expertise of space-faring nations. It has the task to recommend and promote mitigation mission-related research and studies on an international and cooperative level. It develops and adopts a set of reference missions. It develops technical concepts and proposes operational setups. It would also develop applicable decision criteria and timelines. SMPAG is a group of voluntary representatives of space-faring nations. The group calls on support by technical experts and other relevant entities as needed. It provides a yearly summary report to COPUOS. The first meeting of the SMPAG took place in Feb 2014 at the European Space Operations Centre (ESOC) of ESA in Darmstadt, Germany. ESA maintains a web page for the group²².

Response to a credible impact threat

In the case of an actual credible impact threat, the IAWN would provide all available information and updates to COPUOS through the UN Office of Outer Space Affairs. They would also work with disaster response groups in nations that would be affected to prepare and coordinate civil protection plans. The SMPAG would coordinate the space mission planning among space-capable nations. It is suggested that COPUOS may choose to appoint an ad-hoc mitigation advisory group to work together with the response teams.

An example: Suppose that IAWN observes an asteroid where the orbit computations show that there is 20 % chance of an impact in 2050. SMPAG, after performing some mission analysis, proposes as the preferred option for impact mitigation the launch a kinetic impactor/gravity tractor spacecraft combination latest by 2040. This mission would be aimed at deflecting the asteroid. Mission development would need to start in 2030 and would cost about 400 MEuro. As a second option, a kinetic impactor only could be launched in 2028, the mission design could be identical to the already studied 'Don Quixote' mission of ESA. The cost would be 550 MEuro. SMPAG would have the task to evaluate which option to choose and make a proposal on funding and implementation scenarios. COPUOS of the UN would be informed and establish an 'ad-hoc group' or coalition of concerned parties. This coalition could be composed of representatives of countries who would be affected, and of those countries who could actually build and launch a deflection mission. Obviously the two groups don't necessarily have the same members. This coalition would then make proposals to their governments on the actual funding and implementation of a deflection mission.

15. The Planetary Defence Office within the Space Safety programme of the European Space Agency

15.1 Introduction

This section describes the current state (in 2024) of the Planetary Defence Office (PDO) within ESA's Space Safety programme. The Space Safety programme of ESA covers the areas Space Weather, Planetary Defence, and Space Debris and Cleanspace.

15.2 What is Space Safety?

'Space Safety' is defined as the knowledge, understanding and maintained awareness of the (i) population of space objects, of the (ii) space environment, and of the (iii) existing threats/risks.

During the Ministerial Council meeting of the European Space Agency (ESA) in November 2008, the preparatory phase for a so-called European Space Situational Awareness (SSA) system was approved and was funded with about 50 MEuro, which is shared between three segments: Survey and Tracking,

²¹ <http://www.minorplanetcenter.org/IAWN>

²² <http://cosmos.esa.int/SMPAG>

Space Weather, and Near-Earth Objects. In 2012, the project went the so-called 'Period 2' - funded to about the same level for another 4 years until 2016. Period 3 brought the programme to 2019, with a budget of about 90 MEuro. At the Council Meeting on Ministerial Level in Nov 2019, this programme was expanded and renamed to 'Space Safety programme (S2P)'. There are two main elements: The 'core' activities (Space Weather, Planetary Defence, and Space Debris/Cleanspace), and several cornerstone missions: The 'Hera' asteroid deflection demonstration mission for Planetary Defence, an active debris removal demonstration mission (ADRIOS) for the space debris segment, and the preparation for a mission to the Lagrange point #5 in the Sun-Earth system for Space Weather.

15.3 Tasks of the programme

The preparatory phase started in January 2009 and lasted until the end of 2012. During this preparatory phase, precursor services have been set up²³ and thorough studies have been performed to assess the architecture and system requirements. At the end of the preparatory phase, a clear definition of the functional breakdown of the full SSA programme was available. Phase 2 (from Jan 2013 until end of 2016) these breakdowns were further detailed and cost estimates for the full system were developed. After its 'Period 3', the SSA programme was moved to the current Space Safety programme which started in January 2020. For each segment, a *precursor* service is available which, based on existing assets, provides first basic services as required for the segment.

The three segments and their roles were:

- (a) Space Weather - the Sun continuously emits neutral and charged particles, which interact with the electronics of spacecraft and the Earth's ionosphere. In particular after a solar flare the radiation coming from the Sun may be strong enough to disturb the electronic components of a satellite and reduce its functionality. It could also interact with the ionosphere in such a way that *e.g.* signals from the Global Positioning System (GPS) cannot be received properly. Clearly there is a high interest in predicting such events.
- (b) Near-Earth Objects (NEOs) - currently there are more than 35000 NEOs known. Some of them come as close as a few 10000 km to the Earth. It is possible that known objects are deflected by close planetary encounters, or that new objects are discovered which have a high chance of impacting the Earth. Objects larger than about 40 m in diameter will penetrate the Earth's atmosphere and may cause considerable damage.
- (c) Survey and Tracking - covering the survey and tracking of satellites and space debris, *i.e.* man-made objects which are orbiting the Earth. The main contributors to the generation of space debris are collisions between satellites. Space debris may collide with operational satellites and destroy them. A recent example is the collision of a decommissioned Russian Cosmos 2251 satellite with an operational Iridium spacecraft in February 2009. Tracking all satellites including non-operational objects would have allowed predicting the collision and allowing a collision avoidance maneuver of the Iridium spacecraft.

While the roles stay the same, the names have changed. The 'near-Earth object segment' is now called the 'Planetary Defence Office'.

15.4 Detailed tasks of the Planetary Defence Office

The Planetary Defence Office, hereafter called PDO, has the following key tasks:

- It shall provide information on the impact probability and/or miss distances of NEOs including associated uncertainties. To do this properly, it shall assess impact analyses, results, and perform its own impact risk assessments.
- It shall classify the risk of a NEO impact and issue warnings if the risk is higher than the background risk.

²³ The NEO precursor services can be found at <http://neo.ssa.esa.int>

- To perform these tasks, it will set up a network of sensors for the discovery and follow-up observations of asteroids and in particular also for the characterization of these objects. It will also set up data centers for processing the information.
- ESA representatives participate in discussions on the level of the United Nations to set up the political framework for issuing impact warning. In addition, the PDO team maintains close links to groups working on mitigation strategies, e.g. ESA's General Studies Programme.

The main building blocks of the PDO are:

- Network of telescopes. These are mainly optical telescopes, but also radar systems could be involved in the future. In a later phase this can also include space-based telescopes. It includes a measurement, coordination and planning function.
- An NEO Coordination Centre with the following tasks:
 - Perform impact risk computations;
 - Maintain a NEO property database;
 - Support observations to find more NEOs and secure their orbits;
- Interface to studies on risk mitigation;
- Support the decision-making process in case of an imminent impact threat by participating in the UN-endorsed International Asteroid Warning Network (IAWN)²⁴ and the Space Mission Planning Advisory Group (SMPAG)²⁵.

The current top-level architecture of the complete system is depicted in Figure 38.

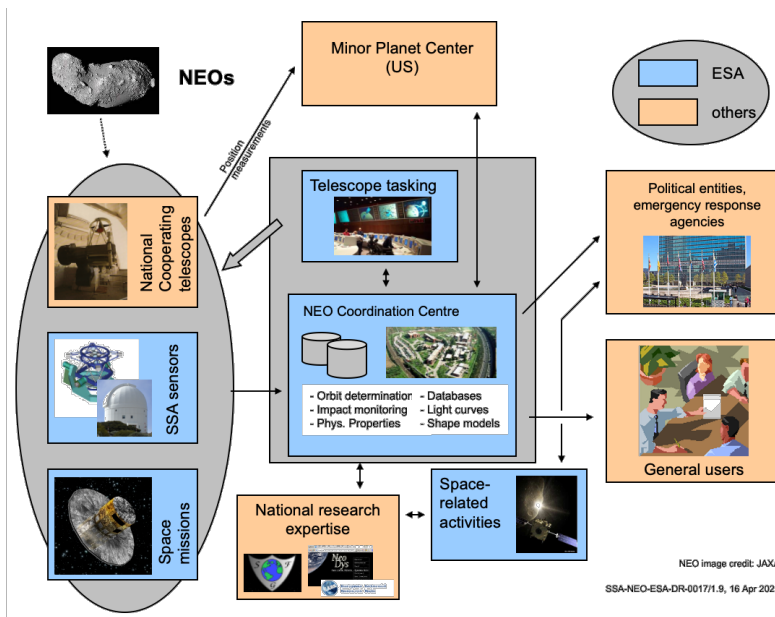


Figure 38: Context diagramme of ESA's Planetary Defence Office.

As measurement infrastructure, a network of instruments is available to ESA's PDO, which combines existing ground-based telescopes. Those in the size range of 0.7 m to 2.2 m aperture are able to perform follow-up observations and photometric measurements of NEOs. Larger telescopes (2.2 m and up)

²⁴ <http://www.iawn.net>

²⁵ <http://www.smpag.net>

would have to be made available for spectroscopic observations needed to determine the spectral type of the object.

An important building block for a telescope network is the coordination of observations. This interface would for example schedule observing time to optimize observation time and avoid that *e.g.* all telescopes would observe the same object. Follow-up observations of newly discovered objects can be enforced actively.

Concerning the data processing infrastructure, the main elements are already available in Europe. However, they need to be transformed and extended from the current state of being an activity of a research center to a real service-providing center. The efforts of the PDO are devoted to standardizing the interfaces and setting up data provision agreements *e.g.* with the Minor Planet Center in the US which is the central collecting place for all asteroid observations world-wide. Note that the final architecture will be a result of studies that are just starting.

Task 8: Apophis will have a close encounter on 13 Apr 2029, with a flyby distance is 0.0002547 AU.

(a) What is the expected brightest magnitude of the object? (Albedo = 0.33, diameter 0.27 km)

(b) What will be the relative flyby velocity? ($a = 0.922296$ au, $e = 0.19109$)

(c) How long will it roughly take to cross half the sky (90 deg)? And the diameter of the Moon (0.5 deg)?

(d) If it did hit – what's the released energy in comparison to the Hiroshima bomb?

Note: Impact energies are often given in 'kilotons TNT' or 'megatons TNT'; 1 kt TNT = $4.184 \cdot 10^{12}$ J. The 'Little Boy' Hiroshima bomb had an explosive yield of 15 kt TNT.

16. Asteroid deflection techniques – avoiding an impact

16.1 Introduction

The following section deals with methods how to deflect an asteroid from its possible impact course. Note that often these deflection missions are referred to as 'mitigation missions'. However, the term 'mitigation' simply means 'to reduce the risk coming from an impact'. Risk is the product of probability times consequence. Impact risk mitigation could thus simply mean to evacuate the area where an impact would be predicted. Therefore we find the term 'mitigation missions' misleading and will use 'deflection mission' instead.

In the following, we distinguish between *impulsive* and *slow push/pull* techniques. Impulsive techniques are those where the momentum change of the asteroid is performed via a short, impulsive, energy transfer. The slow techniques typically have a lower instantaneous force, but act for a long period of time.

16.2 Impulsive deflection

16.2.1 Kinetic impactor

The kinetic impactor is based on the idea that the orbit of the threatening NEO can be changed by impacting it with a large mass. The higher the mass and the velocity of the impactor, the larger the momentum transfer and thus the deflection.

The mathematical assumptions are simple: The change in velocity of an asteroid is described by the conservation of momentum and can be computed by

$$v_{ast} = \beta \frac{m_{imp}}{m_{ast}} v_{imp} \quad (37.)$$

Here, v_{ast} is the velocity of the asteroid, m_{imp} and m_{ast} the mass of the impactor and the asteroid, respectively, v_{imp} the velocity of the impactor. β is called *momentum transfer efficiency*. It describes how much momentum is really transferred between impactor and asteroid.

In the case of an plastic collision with no cratering and resulting ejecta production or fragmentation, $\beta = 1$. In realistic cases, ejecta from the impact may leave the asteroid in the direction opposite the impactor velocity and measured values for β were up to 10. Extrapolating to higher impactor velocities, β would be even higher.

Determining good values for the momentum transfer efficiencies for different projectile and target properties is the goal of several currently ongoing scientific studies, see e.g. Figure 39, Holsapple and Housen (2012), Walker *et al.* (2013).

Task 9: Rosetta (mass about 2 tons) was sent away from the Earth with 3.5 km/s – let's assume we use it to deflect Apophis, when Apophis is at $r = 1$ au during its flyby in 2029. Assume $\beta = 2$ and 20 % loss because of different velocity vector directions. What is the deflection distance after it returns again in 2036?

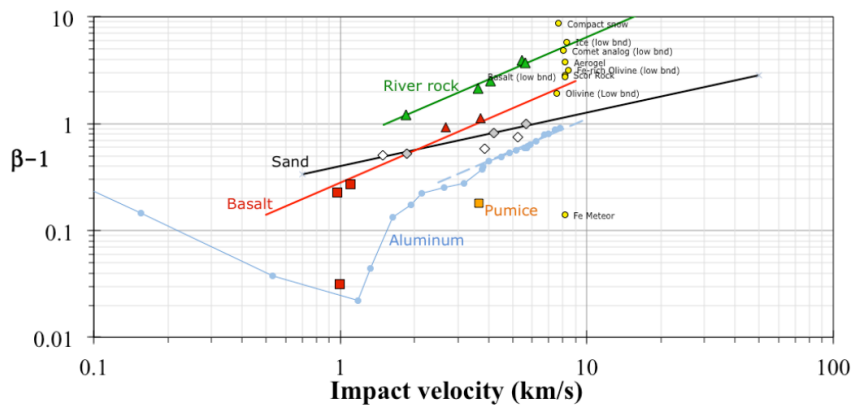


Figure 39: Momentum transfer efficiency for different targets (Holsapple and Housen 2012).

This shows that the effectiveness of a kinetic impactor is very dependent on the properties of the target asteroid. NEOs are expected to be covered with regolith (*i.e.* a mix of individual small rocks with sizes smaller than millimeters up to centimeters). Some asteroids have been shown to have very low bulk

densities of as small as 0.5 g/cm^3 , indicating a high porosity (Baer *et al.* 2011²⁶). The results for sand would seem most appropriate. But to properly predict the deflection of an asteroid precise knowledge of the target must be available.

Another useful formula to allow a quick check of the deflection capabilities was derived by Ahrens and Harris (1994):

$$\Delta s \approx 3\Delta v \cdot t \quad (38.)$$

With this formula, one can estimate the time needed to deflect an asteroid a given distance. Typical lead times are several years to tens of years.

The most detailed study to date analyzing this concept has been ESA's 'Don Quijote' study. A number of technical reports were generated during the time from 2004 to 2007 (Galvez and Carnelli, 2007). Harris *et al.* (2006) summarizes the science return of the project.

Don Quijote²⁷ had the goal to demonstrate the capability of measuring the momentum transfer from an impacting spacecraft to a target asteroid. This would be done by first characterizing the asteroid (2002 AT4), then by measuring changes in its orbit. It would consist of two spacecraft: An orbiter, called Sancho, which would arrive at the asteroid about two months before the impactor. During the time to impact it would orbit the object and characterize it. To do this, it has a model payload containing:

- a camera for taking optical images,
- a laser altimeter measuring the precise size of the object by measuring the distance to the spacecraft,
- an infrared spectrometer determining the mineralogical composition of (at least the surface of) the asteroid,
- a thermal infrared imager allowing to determine the temperature and with that the thermal inertia of the asteroid; this in turns allows estimating properties like porosity or thickness of a possible surface regolith,
- an x-ray spectrometer and a radiation monitor measuring atomic composition of the surface,
- a radio science experiment which allows via very precise radio tracking of the spacecraft the determination of its relative position.

The radio science experiment is used to determine the mass of the asteroid by measuring the orbit of the spacecraft relative to the asteroid. Using the optical camera and the laser altimeter allows to measure size and shape of the object. With these two measurements, the bulk density of the asteroid can be measured. Together with the other instruments, the composition and structure of the object can be quite well constrained. The orbiter would also carry a so-called Autonomous Surface Package. This is a small spacecraft that would be deployed from the orbiter and land on the surface after the impact, possibly in the fresh impact crater. Some small in-situ instruments (a Mössbauer spectrometer, a mass spectrometer, a micro camera and a thermal sensor) would perform more detailed measurements of the touch-down site.

In the baseline mission scenario, the impactor, called Hidalgo, would hit the asteroid at a relative velocity of about 10 km/s. The total wet mass of the impactor would be about 1.7 t; upon arrival it would have exhausted its fuel and have a mass of about 530 kg. It has a small payload containing mainly of an optical navigation system which guides the impactor into the target.

After the impact, the orbiter will deploy the surface experiment system. It will stay in orbit around the asteroid and, via the radio science experiment, allow a very precise determination of the asteroid orbit. The mission was designed such that it could measure a possible deflection to at least 10 % accuracy.

²⁶ They have studied the mutual perturbations of asteroids in the main belt and from that derived the rough masses for 26 objects. Combining this with size estimates from other objects leads to the bulk density.

²⁷ http://www.esa.int/Our_Activities/Technology/NEO/Don_Quijote_concept

Task 11: Take the binary asteroid 1996FG3. The distance between the two components is 2.8 km. Assume a circular orbit. What is the orbital period? Assume an asteroid density of 1.4 g/cm^3 and a momentum efficiency of $\beta = 2$.

Assume that the Deep Impact impactor hits the secondary (370 kg, 10.2 km/s). By how much do you change the period? How can this be measured?

This study was performed in the General Studies Programme of ESA. It was not proposed for actual implementation, but led into a follow-up study called AIDA (Asteroid Impact & Deflection Assessment) study (Cheng *et al.* 2012).

The AIDA study started around 2010 and is a collaboration between ESA²⁸ and NASA. The NASA part, DART (Double-Asteroid Redirection Test), is under construction since 2018. The ESA contribution, Hera, has been selected for flight at the end of 2024. DART launched in 2021 to impact the smaller object of the double asteroid Didymos in October 2022. The impact was successful and changed the orbit of asteroid Dimorphos around its parent body Didymos from about 12 hours period to 11 hours and 30 minutes (more to be written, give references). Hera will arrive at the system in 2026 (tbc) and characterize the surface of the objects and the impact crater.

16.2.2 Nuclear methods

To be written.

16.3 Slow-push or -pull techniques

16.3.1 Gravity tractor

To be written.

16.3.2 Ion-beam shepherd

To be written.

16.4 Other concepts

The previous mission concepts are those which seem currently feasible. However, a number of more 'exotic' concepts have been proposed.

The *mass driver* concept would put a lander on the asteroid which takes material from the surface and accelerates it away from the asteroid. The resulting thrust would move the object. This concept faces several challenges. How to remove large quantities of mass from the asteroid surface is not really clear. Also, the masses should only be accelerated away from the asteroid when the orientation is correct. This is one of the most exotic concepts.

The *mirror-bee* concept is proposing to use a number of mirrors to reflect sunlight onto the asteroid's surface. Given enough mirrors, the surface can be heated up enough to sublimate. The sublimation will generate a pressure onto the surface, acting like a thruster and pushing the asteroid away.

Other concepts have been proposed. However, the kinetic impactor, gravity tractor, and ion-beam shepherd are considered the most promising ones by the authors.

²⁸ http://www.esa.int/Our_Activities/Technology/NEO/Asteroid_Deflection_Assessment_AIDA_study

Task 10: The first impact demonstration was done by the Deep Impact mission. A 350 kg projectile hit a comet with 10.2 km/s. The comet has a size of about $8 \times 5 \times 5$ km³.

What are reasonable assumptions for the momentum transfer coefficient β ?

What is the velocity change (assume a reasonable β)?

Assume the comet is hit in apocenter – how much later does it arrive at pericentre compared to without hit? What distance does that correspond to? Use the values $a = 3.12404524$ au and $e = 0.516946$ for the comet orbit.

17. References

- Alvarez, L. W., Alvarez, W., Asaro, F., Michel, H. V., Extraterrestrial Cause for the Cretaceous-Tertiary Extinction. *Science* **208:4448** (1980).
- Baer, J., Chesley, S. R., Matson, R. D., Astrometric masses of 26 asteroids and observations on asteroid porosity, *The Astronomical Journal* **141:143**, 1-12 (2011).
- Bancelin, D., Etude de la dynamique des asteroides geocroiseur, Ph.D. thesis, Paris Observatory (2011).
- Bate, R. R., Mueller, D. D., White, J. E., Fundamentals of Astrodynamics, Dover Publications, Inc., New York, ISBN 0-486-60061-0 (1971).
- Berry, R., Burnell, J., The Handbook of Astronomical Image Processing 2.0, Willmann-Bell, Inc., Richmond, VA, ISBN 0-943396-82-4 (2006).
- Brown, P., and 32 coauthors, A 500-kiloton airburst over Chelyabinsk and an enhanced hazard from small impactors, *Nature* **503:7475**, 238-241 (2013).
- Buchheim, R. K., The sky is your laboratory, Springer (2007).
- Cheng, Andrew F.; Rivkin, A.; Galvez, A.; Carnelli, I.; Michel, P.; Reed, C., AIDA: Asteroid Impact & Deflection Assessment, American Astronomical Society, DPS meeting #44, Abstract #215.03.
- Chesley *et al.*, Quantifying the risk posed by potential Earth impacts, *Icarus* **159**, 423-432 (2002).
- Collins, Melosh, Marcus, Earth Impact Effects Program, *Meteoritics & Planetary Space Science* **40:6**, 817-840 (2005).
- Cousins, A. W. J., VRI Standards in the E Regions, *Memoirs of the Royal Astronomical Society* **81**, 25-36 (1976).
- DeMeo, F., Binzel, R. P., Slivan, S. M., Bus, S. J., An extension of the Bus asteroid taxonomy into the near-infrared, *Icarus* **202**, Issue 1, p. 160-180 (2009).
- Galvez, A., Carnelli, I., Learning to deflect near-Earth objects: industrial design of the Don Quijote mission. 57th International Astronautical Congress, Valencia, Spain. Abstract No. IAC-06-A03.5.05 (2006).
- Granvik, M., Morbidelli, A., Jedicke, R., Bolin, B., Bottke, W. F., Beshore, E., Vokrouhlicky, D., Nesvorny, D., Michel, P., Debaised orbit and absolute-magnitude distributions for near-Earth objects, *Icarus*, **312**, 181-207 (2018).
- Harris, A. W.; Galvez, A.; Benz, W.; Fitzsimmons, A.; Green, S. F.; Michel, P.; Valsecchi, G.; Paetzold, M.; Haeusler, B.; Carnelli, I., Mitigation-relevant science with Don Quijote - a European-led mission to a near-Earth asteroid, 36th COSPAR Scientific Assembly, 16-23 Jul 2006, Beijing, China.
- Harris, A. W., Drube, L., How to find metal-rich asteroids, *The Astrophysical Journal Letters* **785:L4**, 1-5 (2014).
- Holsapple, K., Housen, K. R., Momentum transfer in asteroid impacts. I. Theory and scaling, *Icarus* **221/2**, 875-887 (2012).
- Jansson, K. W., Johansen, A., Bukhari Syed, M., Blum, J., The role of pebble fragmentation in planetesimal formation. II. Numerical simulations. *Astrophys. J.* **835**, 109-120 (2017).
- Johnson, H. L., Morgan, W. W., Fundamental stellar photometry for standards of spectral type on the Revised System of the Yerkes Spectral Atlas, *Astrophys. J.* **117**, 313 (1953).
- Koschny, D. MarcoPolo-R programatics, science requirements, and engineering requirements for target characterization, presented at the 2nd MarcoPolo-R workshop on Physical Characterization of MarcoPolo-R Targets, Meudon, France, 12-13 Jan 2012 (available at <http://smass.mit.edu/MarcoPolo/program.html>).

Koschny, D., Soja, R. H., Engrand, C., Flynn, G. J., Lasue, J., Levasseur-Regourd, A.-C., Malaspina, D., Nakamura, T., Poppe, A., R., Sterken, V. J., Trigo-Rodriguez, J. M., Interplanetary dust, meteoroids, meteors and meteorites, *Space Science Reviews* **215**, 34 (2019).

Koschny, D., Borovicka, J., Definitions of terms in meteor astronomy, *WGN, J. Int. Met. Org.* **45:5**, 91-92 (2017).

Koschny, D. and Busch, M., The Teide Observatory Tenerife Asteroid Survey, *Planet. Space Sci.* **118**, 305-310 (2015).

Lebofsky, L. A., Sykes, M. V., Tedesco, E. F., Veeder, G. J., Matson, D. L., Brown, R. H., Gradie, J. C., Feierberg, M. A., Rudy, R. J., A refined 'standard' thermal model for asteroids based on observations of 1 Ceres and 2 Pallas, *Icarus* **68**, 239-251 (1986).

Muinenon, K., Belskaya, I. N., Cellino, A., Delbo, M., Levasseur-Regourd, A.-C., Penttilä, A., Tedesco, E. F., A three-parameter magnitude phase function for asteroids, *Icarus* **209**, 542-555 (2010).

NASA – Near-Earth object survey and deflection analysis of alternatives, report to congress, Mar 2007 (http://www.nasa.gov/pdf/171331main_NEO_report_march07.pdf).

O'Dell, C. R., Wen, Z., Hu, X., Discovery of new objects in the Orion nebula on HST images: Shocks, compact sources, and protoplanetary disks. *Astrophys. J.* **410**, 696-700 (1993).

Öpik, E. J., Proc. Roy. Irish Acad. **54** (1951), 165

Peebles, C., Asteroids: a history, ISBN 1-56098-389-2, Smithsonian Institution (2000).

Pfalzner, S., Bavies, M. B., Gounelle, M., Johansen, A., Münker, C., Lacerda, P., Portegies Zwart, S., Testi, L., Triaelloff, M., Veras, D., The formation of the solar system, *Phzsica Scripta* **90:6** (2015).

Tancredi, G., Ishitskuka, J., Rosales, D., Vidal, E., Dalmau, A., Pavel, D., Benavente, S., Mrainda, P., Pereira, G., Vallejos, V., Varela, M.E., Brandstätter, F., Schultz, P., Harris, R.S., Sanchez, L., What do we know about the "Carancas-Desaguadero" fireball, meteorite, and impact crater?, *Lunar and Planetary Science Conference XXXIX*, abstract no. 1216 (2008).

Johnson, H.L., and Morgan, W.W. "Fundamental Stellar Photometry for Standards of Spectral Type on the Revised System of the Yerkes Spectral Atlas." *The Astrophysical Journal* **117** (May 1953): 313–352.

Vokrouhlický, D., Diurnal Yarkovsky effect as a source of mobility of meter-sized asteroidal fragments, *Astron. Astrophys.* **335**, (1998), 1093-1100.

Walter, U., *Astronautics*, Wiley-VCH Verlag GmbH & Co. KGaA (2008).

Walker, J. D., Chocron, S., Durda, D. D., Grosch, D. J., Movshovitz, N., Richardson, D. C., Asphaug, E., Momentum enhancement from aluminum striking granite and the scale size effect, *Int. J. Impact Eng.* **56**, 12-18 (2013).

18. Acronyms

ASCII	American Standard Code for Information Interchange
ASE	Association of Space Explorers
AU	Astronomical Unit (distance Earth-Sun = 149.8 Mio km)
CCD	Charged-Coupled Device (a sensor converting photons in electrons)
COPUOS	Committee on the Peaceful Uses of Outer Space
CRECTEALC	Regional Center for Education in Space Science and Technology in Latin America and the Caribbean
CSS	Catalina Sky Survey (a US asteroid survey program)
DLR	Deutsche Forschungsanstalt für Luft- und Raumfahrt
EARN	European Asteroid Research Node
ESA	European Space Agency

ESRIN	European Space Research Institute
FITS	Flexible Image Transport System
IAU	International Astronomical Union
IAWN	International Asteroid Warning Network
INAF	Istituto Nazionale di Astrofisica (National institute for astrophysics, Italy)
JPL	Jet Propulsion Laboratory
LSSS	La Sagra Sky Survey
MBO	Main-Belt Object (asteroid or comet)
MOID	Mean Orbital Intersection Distance (shortest distance between two orbits)
MPEC	Minor Planet Electronic Circular
MPOG	Mission Planning and Operations Group
NASA	National Aeronautics and Space Administration
NEO	Near-Earth Object (asteroid or comet)
NEODyS	NEO Dynamics Site
OOSA	Office for Outer Space Affairs
Pan-STARRS	Panoramic Survey Telescope & Rapid Response System
PS	Palermo scale value (a measure for the risk an asteroid poses)
SMPAG	Space Missions Planning Advisory Group
SOI	Sphere of Influence
SQL	Structured Query Language
SSA	Space Situational Awareness
SST	Survey and Tracking (one of the segments of ESA's SSA programme)
TIRA	Tracking and Imaging Radar (in Germany, close to Bonn)
TNT	Trinitrotoluol (an explosive)
TOTAS	Teide Observatory Tenerife Asteroid Survey
UN	United Nations
USA	United States of America



Figure 40: This is not a near-Earth object, but a main belt asteroid. Asteroid Lutetia as imaged by the OSIRIS camera onboard ESA's Rosetta spacecraft, on 10 Jul 2010. Image credit: ESA 2011 MPS for OSIRIS Team MPS/UPD/LAM/IAA/RSSD/INTA/UPM/DASP/IDA.

19. Tasks

19.1 Task 1 - Telescope image scale

Take ESA's OGS (Optical Ground Station) telescope on Tenerife. The main mirror has 1 m in diameter. For asteroid observations, it is used in an $f/4.4$ configuration. The CCD camera used has a pixel size (see next section) of $15\ \mu\text{m}$. What is the image scale per pixel?

19.2 Task 2 - Telescope sensitivity

Task 2: The camera at ESA's telescope on Tenerife is cooled by liquid nitrogen to temperatures such that the dark current and its noise contribution can be neglected. The readout is slow enough so that also its noise contribution can be neglected. The camera is operated with a bias of $DN_{bias} \sim 4000$.

For a reliable detection, the SNR of an object should be larger than 5. Compute the sensitivity of ESA's telescope in magnitude, as described in Task 2, using the following assumptions for the CCD camera: $QE = 80\%$; $g = 0.9\ e^-/DN$. Assume that all the photons coming from the object are red at a wavelength of 600 nm. Assume that the telescope transmits $\tau = 80\%$ of the photons to the CCD; $p_{px} = 10\%$ of the photons fall on the center pixel. The telescope obstruction is 10% of the size of the main mirror.

19.3 Task 3 - Palermo scale values

Task 3: The asteroid 2008 TC₃ entered the Earth's atmosphere over Sudan in Oct 2008 and exploded in about 20 km altitude. A number of meteorites were found which came from the object. Its estimated size corresponds to a sphere of radius 4 m. Its velocity was measured in space to be 15 km/s relative to the Earth. The density of the meteorites recovered after the explosion was around $2.5\ \text{g/cm}^3$.

Assume that the complete kinetic energy was converted into explosive energy. How many Hiroshima bombs would be needed to generate the same explosive force?

Task 4: What would have been the Palermo scale (PS) value of this object one year before the impact? What is the PS value of the currently most dangerous object? Check on the NEODYs 'risk page'. Would the Sudan event have a higher or a lower value?

19.4 Task 4: Temperature of an asteroid

Task 4: Using the Stefan-Boltzmann law and the 'Standard Thermal Model', estimate the temperature of an asteroid at 1 AU and 2 AU distance to the Sun. Assume the emissivity ϵ of regolith: 1.0; use albedo $A = 0.04$ (primitive asteroid) and 0.4 (Steins).

19.5 Task 5: Radar equation

Task 5: Assume that for 'imaging', the Arecibo radio antenna needs to be able to detect at least $P_{received} = 1e-16\ \text{W}$. What is the largest distance in which it can image an asteroid with 100 m size?

As an emitter, the Goldstone antenna is used. It has a 400 kW emitter (effectively $P_S = 400\ \text{GW}$ in pulsed mode). The gain is 80 dB. The effectivity of the Arecibo receiver is $K_a = 0.7$, its diameter 300 m.

19.6 Task 6: Asteroid movement

(a): What is the typical angular velocity in arcsec/min of a main-belt asteroid as seen from the Earth when the object is in opposition?

Assume a distance to the Sun of 2.5 AU, circular orbit

(b): ESA's 1-m telescope is an $f/4.4$ system. The CCD camera has a pixel scale of $13.5\ \mu\text{m}$. If you want to limit the image smear to less than 1.5 pixel, how long can your maximum exposure time be?

(c): How long will it take for a main-belt object of 100 m and average thermal conductivity and $a = 2.2\ \text{AU}$ to drift to the next resonance?

(d): What is needed to predict the Yarkowsky effect?

19.7 Task 7: Position of an asteroid

Write a 'program outline' to compute the position of an asteroid, given its orbital parameters

Perform the computation for an object with $a = 1.5$ AU, $e = 0.5$

- How much time does the object spend between 0.983 and 1.02 AU?

19.8 Task 8: The Apophis story

Apophis will have a close encounter on 13 Apr 2029, with a flyby distance is 0.0002547 AU.

(a) What is the expected brightest magnitude of the object? (Albedo = 0.33, diameter 0.27 km)

(b) What will be the relative flyby velocity? ($a = 0.922296$ AU, $e = 0.19109$)

(c) How long will it roughly take to cross half the sky (90 deg)? And the diameter of the Moon (0.5 deg)?

(d) If it did hit – what's the released energy in comparison to the Hiroshima bomb?

- Impact energies are often given in 'kilotons TNT' or 'megatons TNT'
 - 1 kt TNT = 4.184×10^{12} J
- The 'little boy' Hiroshima bomb had an explosive yield of 15 kt TNT

19.9 Task 9: Apophis deflection

Rosetta (mass about 2 tons) was sent away from the Earth with 3.5 km/s – let's assume we use it to deflect Apophis, when Apophis is at $r = 1$ AU during its flyby in 2029. Assume $b = 2$ and 20 % loss because of different velocity vector directions.

What is the deflection distance after it returns again in 2036? Use the following approximation: $D_s = 3 \times D_v \times t$ (Chesley 2005).

19.10 Task 10: The Deep Impact mission

So far the only impact demonstration was done by the Deep Impact mission. A 350 kg projectile hit the comet with 10.2 km/s. The comet has a size of about $8 \times 5 \times 5$ km³.

What are reasonable assumptions for the momentum transfer coefficient b ?

What is the velocity change (assume a reasonable b)?

Assume the comet is hit in apocenter – how much later does it arrive at pericenter compared to without hit? What distance does that correspond to? Use the values $a = 3.12404524$ AU and $e = 0.516946$ for the comet orbit.

19.11 Task 11: Impact deflection demonstration using a binary asteroid

Take the binary asteroid 1996FG3. The distance between the two components is 2.8 km. Assume a circular orbit. What is the orbital period? Assume an asteroid density of 1.4 g/cm³ and a momentum efficiency of $b = 2$.

Assume that the Deep Impact impactor hits the secondary (370 kg, 10.2 km/s). By how much do you change the period? How can this be measured?

19.12 Task 12: The Ion-Beam Shepherd

Let's assume that we want to use two Smart-I spacecraft mounted 'back-to-back' as Ion-Beam Shepherd. Using the data sheet of the S-1 ion engine (*), where would you put the spacecraft? How much do you shift Apophis after one year/two years/ten years/twenty years?

The data sheet for the ion thrusters can be found here:

http://www.snecma.com/IMG/files/fiche_pps1350g_ang_2011_modulvoir_file_fr.pdf.

20. Acknowledgements

This text has been written over the several years and has been constantly improved. It is still far from perfect... But anyway, I thank the students of the 2011 course for their thorough review. The section on the nu6 resonance was checked by P. Michel. All images which don't have explicit credit are by D. Koschny.